Article:
Pecci, A, Klersy, C, Gresele, P et al. (2014) MYH9-related disease: A novel prognostic model to predict the clinical evolution of the disease based on genotype-phenotype correlations. Human Mutation, 35 (2). pp. 236-247. ISSN: 1059-7794

https://doi.org/10.1002/humu.22476

MYH9-RELATED DISEASE: A NOVEL PROGNOSTIC MODEL TO PREDICT THE CLINICAL EVOLUTION OF THE DISEASE BASED ON GENOTYPE-PHENOTYPE CORRELATIONS

Alessandro Pecci ,[1] Catherine Klersy,[2] Paolo Gresele,[3] Kieran J.D. Lee,[4] Daniela De Rocco,[5] Valeria Bozzi,[1] Giovanna Russo,[6] Paula G. Heller,[7] Giuseppe Loffredo,[8] Matthias Ballmaier,[9] Fabrizio Fabris,[10] Eloise Beggiato,[11] Walter HA Kahr,[12] Nuria Pujol-Moix,[13], Helen Platokouki,[14] Christel Van Geet,[15] Patrizia Noris,[1] Preethi Yerram,[16], Cedric Hermans,[17] Bernhard Gerber,[18] Marina Economou,[19] Marco De Groot,[20] Barbara Zieger,[21], Erica De Candia,[22] Vincenzo Fraticelli,[23]Rogier Kersseboom,[24] Giorgina B. Piccoli,[25] Stefanie Zimmermann,[26] Tiziana Fierro,[3] Ana C. Glembotsky,[7] Fabrizio Vianello,[10] Carlo Zaninetti [1], Elena Nicchia,[5] Christiane Güthner,[27]Carlo Baronci,[28] Marco Seri,[29] Peter J. Knight,[4] Carlo L. Balduini,[1] Anna Savoia.[5,30]

[1] Dept. of Internal Medicine, IRCCS Policlinico San Matteo Foundation and University of Pavia, Italy; [2] Service of Biometry & Statistics, IRCCS Policlinico San Matteo Foundation, Pavia, Italy; [3] Dept. of Internal Medicine, Section of Internal and Cardiovascular Medicine, University of Perugia, Italy; [4] Astbury Centre for Structural Molecular Biology, School of Molecular and Cellular Biology, University of Leeds, United Kingdom; [5] Dept. of Medical Sciences, University of Trieste, Italy; [6] Division of Pediatric Hematology/Oncology, University of Catania, Italy; [7] Dept. of Hematology Research, Instituto de Investigaciones Médicas Alfredo Lanari, UE IDIM-CONICET, University of Buenos Aires, Argentina; [8] Dept. of Oncology, Azienda "Santobono-Pausilipon", Pausilipon Hospital, Napoli, Italy; [9] Pediatric Hematology and Oncology, Hannover Medical School, Hannover, Germany; [10] Dept. of Medicine-DIMED, University of Padova Medical School, Padova, Italy; [11] Dept. of Hematology-Oncology, Hospital "Città della Salute e Della Scienza", Torino, Italy; [12] Dept. of Paediatrics and Biochemistry, University of Toronto, Division of Hematology/Oncology, The Hospital for Sick Children, Toronto, Canada; [13] Institut d'Investigació Biomèdica Sant Pau, Universitat Autònoma de Barcelona, Spain; [14] Haemophilia Centre and Haemostasis Unit, "Aghia Sophia" Children's Hospital, Athens, Greece; [15] Center for Molecular and Vascular Biology, University of Leuven, Belgium; [16] Dept. of Internal Medicine, University of Missouri-Columbia School of Medicine, Columbia, MO, USA; [17] Division of Hematology, St-Luc University Hospital, Brussel, Belgium; [18] Division of Hematology, University Hospital Zurich, Switzerland; [19] Pediatric Hematology, Aristotle University, Thessaloniki, Greece; [20] Dept. of Hematology, University Medical Center Groningen, The Netherlands; [21] Dept. of Pediatrics and Adolescent Medicine, University Medical Center Freiburg, Germany; [22] Dept. of Internal Medicine, Catholic University of Rome, Italy; [23] Hematology Unit, Giovanni Paolo II Foundation, Campobasso, Italy; [24] Dept. of Clinical Genetics, Erasmus Medical Centre, Rotterdam, The Netherlands; [25] Dept. of Clinical and Biological Sciences, University of Torino, Italy; [26] Pediatric Hematology and Oncology, J.W. Goethe-University, Frankfurt, Germany; [27] Dept. of Medical Oncology and Hematology, Stadtspital Triemli, Zurich, Switzerland; [28] Dept. of Pediatric Hematology and Oncology, Pediatric Hospital "Bambino Gesù", Rome, Italy; [29] Medical Genetics Unit, Policlinico Sant'Orsola-Malpighi, University of Bologna, Bologna, Italy; [30] Institute for Maternal and Child Health, IRCCS "Burlo Garofolo", Trieste, Italy.

Corresponding author:

Alessandro Pecci, MD, PhD, Dept. of Internal Medicine, IRCCS Policlinico San Matteo Foundation and University of Pavia, Piazzale Golgi, 27100 Pavia. Tel: +39.0382.501385; Fax: +39.0382.526223; e-mail: alessandro.pecci@unipv.it

ABSTRACT

MYH9-related disease (*MYH9*-RD) is a rare autosomal-dominant disorder caused by mutations in the gene for non-muscle myosin heavy chain IIA (NMMHC-IIA). *MYH9*-RD is characterized by a considerable variability in clinical evolution: patients present at birth with only thrombocytopenia, but some of them subsequently develop sensorineural deafness, cataract, and/or nephropathy often leading to end-stage renal disease (ESRD). We searched for genotype-phenotype correlations in the largest series of consecutive *MYH9*-RD patients collected so far (255 cases from 121 families). Association of genotypes with non-congenital features was assessed by a generalized linear regression model. The analysis defined disease evolution associated to seven different *MYH9* genotypes that are responsible for 85% of *MYH9*-RD cases. Mutations hitting residue R702 demonstrated a complete penetrance for early-onset ESRD and deafness. The p.D1424H substitution associated with high risk of developing all the non-congenital manifestations of disease. Mutations hitting a distinct hydrophobic seam in the NMMHC-IIA head domain or substitutions at R1165 associated with high risk of deafness but low risk of nephropathy or cataract. Patients with p.E1841K, p.D1424N and C-terminal deletions had low risk of non-congenital defects. These findings are essential to patients' clinical management and genetic counseling and are discussed in view of molecular pathogenesis of *MYH9*-RD.

Key Words: *MYH9*-related disease, non-muscle myosin, inherited thrombocytopenia, genetic nephropathy, genetic deafness.

INTRODUCTION

MYH9-related disease (*MYH9*-RD) is an autosomal-dominant disorder caused by mutations in *MYH9* (OMIM 160775), the gene for the heavy chain of non-muscle myosin IIA (NMMHC-IIA) [Kelley et al., 2000; Seri et al., 2000; Kunishima et al., 2001]. *MYH9*-RD patients present at birth with thrombocytopenia and platelet macrocytosis. The degree of thrombocytopenia is greatly variable among different subjects and the reduced platelet count can associate with mild to severe bleeding tendency. Most *MYH9*-RD patients develop, during infancy or adult life, additional clinical manifestations: sensorineural deafness, presenile cataract, and/or proteinuric nephropathy, which usually evolves into kidney failure and often leads to end-stage renal disease (ESRD). Each of these non-congenital manifestations can occur alone or can variably associate with the other ones. Therefore, clinical evolution of *MYH9*-RD is extremely variable: in some patients, a mild, asymptomatic thrombocytopenia remains the only manifestation of the disease throughout life, while other subjects develop over time complex syndromic pictures characterized by spontaneous bleedings, ESRD, deafness and/or cataract [Balduini et al., 2011; Kunishima and Saito, 2010]. *MYH9*-RD encompasses four syndromes that have been considered for many years as distinct disorders, May-Hegglin Anomaly (MHA, MIM 155100), Sebastian syndrome (SBS, MIM 605249), Fechtner syndrome (FTNS, MIM 153640), and Epstein syndrome (EPTS, MIM 153650). After the discovery of *MYH9* as the gene responsible for all of these syndromes, analyses of wide case series of patients demonstrated that MHA, SBS, FTNS and EPTS actually represented some of the different possible clinical presentations of the same condition, for which the definition of *MYH9*-RD, or *MYH9* disorder, has been introduced [Seri et al., 2003; Heath et al., 2001; Arrondel et al., 2002; Althaus and Greinacher, 2009; Kunishima and Saito, 2010; Balduini et al., 2011].

Non-muscle myosin-IIA is a cytoplasmic myosin expressed in most cell types and tissues that participates in several key processes requiring generation of chemomechanical forces by the cytoskeleton, such as cell motility, cytokinesis, cell polarization and maintenance of cell shape [Vicente-Manzanares et al., 2009]. Like all conventional myosins, it presents a hexameric structure formed by a NMMHC-IIA dimer and two pairs of light chains. Each NMMHC-IIA molecule comprises three anatomically distinct domains: the N-terminal

globular head domain (HD), the light chain binding lever arm or neck, and the C-terminal tail domain (TD) [Eddinger and Meer, 2007] (**Supp. Figure S1, B**). The three-dimensional structure of the globular HD consists of four subdomains connected by flexible linkers: the N-terminal SH3-like motif, the upper and the lower 50kDa subdomains, and the converter subdomain [Sellers, 2000] (**Supp. Figure S2**). The so-called motor domain includes the highly-conserved functional regions essential for production of chemomechanical force, such as the actin-binding cleft, the ATP-binding pocket, the relay loop, and the short SH1 helix [Dominguez et al.,1998; Sweeney and Houdusse, 2010; Baumketner, 2012]. The TD comprises two regions: a long alpha-helical coiled-coil, which connects two NMMHC-IIA moieties to form one dimer and represents the binding site of different dimers to form functional myosin filaments, and a 37-residue C-terminal non-helical tailpiece (NHT), which is a phosphorylation site with regulatory functions [Eddinger and Meer, 2007; Sanborn et al., 2011] (**Supp. Figure S1**).

The spectrum of mutations identified so far in *MYH9*-RD is limited, suggesting that only specific alterations of NMMHC-IIA cause the disease. In most patients, *MYH9*-RD is due to missense mutations affecting either the HD or the coiled-coil region of the TD. Missense mutations hit only 21 of the 1960 NMMHC-IIA residues [Balduini et al., 2011; De Rocco et al., 2013]. In other patients, *MYH9*-RD derives from nonsense or frameshift alterations of the last exon (exon 41) resulting in deletion of a variable portion of the NHT. In rare cases, the causative mutation is an in-frame deletion or duplication removing or adding short amino acid sequences, mainly within the C-terminal part of the coiled-coil. In about 80% of the families, the mutations affected six residues: S96 or R702 located in the HD, R1165, D1424 or E1841 in the coiled-coil, or R1933 in the NHT [Balduini et al., 2011].

Due to the large variability of the clinical picture, the search for genotype-phenotype correlations in *MYH9*-RD has been an important research topic since the identification of this disorder [Seri et al., 2003; Althaus and Greinacher, 2009; Kunishima and Saito, 2010]. In 2005, Dong and colleagues suggested a relationship between mutations of some NMMHC-IIA residues and the phenotypes of the respective families [Dong et al., 2005]. In 2008, the analysis of 108 patients enrolled in the Italian registry for *MYH9*-RD showed that the mutations affecting the HD of NMMHC-IIA were associated with a higher incidence of nephropathy and

deafness and with more severe thrombocytopenia than mutations hitting the TD [Pecci et al., 2008a]. Some of the reports on very small case series published afterwards were consistent with this model based on HD vs. TD contraposition [Pecci et al., 2010; Sekine et al., 2010; Han et al., 2011], while others suggested the need for a more articulate prognostic model [De Rocco et al., 2009; Jang et al., 2012].

After the first genotype-phenotype study published in 2008, the number of patients enrolled in the Italian registry rose from 108 to 255 and the observation time increased by more than 5 years. The analysis of this very large case series showed that different mutations within the same NMMHC-IIA domain, and even hitting the same residue, can have different effects on phenotype, thus allowing us to define a novel and more accurate prognostic model.

PATIENTS AND METHODS

Patients

This study included all the consecutive patients enrolled in the Italian Registry for *MYH9*-RD (www.registromyh9.org) at the date of March 2012. **Supp. Figure S3** describes in detail the protocol used for patients' enrollment. Patients having the inclusion criteria were recruited at the different centers participating in the registry network. All patients or their legal guardians provided written informed consent. The study was approved by the Institutional Review Board of the IRCCS Policlinico San Matteo Foundation, Pavia, Italy.

Immunofluorescence assay

Immunofluorescence assay for the search for NMMHC-IIA leukocyte inclusions on the peripheral blood smears was performed in all the consecutive unrelated probands with inclusion criteria (**Supp. Figure S3**). This assay was used as a screening test on the basis of the previous evidences indicating that it represents the most sensitive method to identify patients with *MYH9*-RD [Savoia et al., 2010; Althaus and Greinacher,

2010; Kunishima et al., 2003; Kunishima and Saito, 2010]. In particular, the assay demonstrated a 100% sensitivity for the identification of subjects with *MYH9* mutations [Savoia et al., 2010]. The immunofluorescence assay was centralized at the laboratory of the Department of Internal Medicine, IRCCS Policlinico San Matteo Foundation, Pavia. The test was performed using the anti-NMMHC-IIA mouse monoclonal antibody NMG2 according to a previously reported protocol [Savoia et al., 2010].

Mutational screening of *MYH9*

Mutational screening of *MYH9* was centralized at the laboratories of Institute for Maternal and Child Health, IRCCS "Burlo Garofolo", Trieste, Italy or of the Medical Genetics Unit, Policlinico Sant'Orsola-Malpighi, University of Bologna, Bologna, Italy. The analysis was performed using a tiered approach based on localization and frequency of mutations so far detected [Savoia et al., 2010]. First, we took into consideration exons 2, 17, 31, 39, and 41. If no mutation was identified, screening was extended to exons 11, 21, 25, 26, 27, 32, 33, 35, and 38. In some patients, the analysis was extended to all the *MYH9* coding exons. The coding exons and the respective exon-intron boundaries were amplified by PCR as described [Savoia et al., 2010]. PCR products were sequenced using an ABI PRISM BigDye Terminator Cycle Sequencing Ready Reaction Kit and an ABI 310 Genetic Analyzer (Applied Biosystems, Foster City, CA, USA). Nucleotide numbering reflects the *MYH9* cDNA with +1 corresponding to the A of the ATG translation initiation codon in the reference sequence (RefSeq NM_002473.4). Therefore, the initiation codon is codon 1. All the mutations are enlisted in a locus specific mutation database (http://www.LOVD.nl/MYH9) at the Leiden Open Variation Database.

Phenotype assessment

Patients were studied at diagnosis and then reevaluated at least once a year. Patients' age used for the analysis was that at the time of the last clinical evaluation. The phenotype of the already reported patients was updated for this study. Proteinuric nephropathy was recorded when quantitative 24-hours proteinuria was more than 0.5 gr in at least two consecutive examinations repeated with an interval of three months.

Chronic renal failure (CRF) was recorded in patients with proteinuric nephropathy for values of serum creatinine at least 1.5-fold higher than the upper reference value or an estimated GRF < 60 mL/min/1.73 m^3 according to the CKD-EPI creatinine equation [Levey et al., 2009], in at least two consecutive examinations. ESRD was defined by the need for continuous dialysis. The presence of sensorineural hearing loss was defined on the basis of the results of audiometric examination. Deafness was recorded for a bone threshold average greater than 25 dB at 1000, 2000 and 4000 Hz. For infants the hearing function was examined by sensory evoked potentials. Presenile cataract was searched for by ophthalmological evaluation. In most cases, the automated or microscopic platelet count was repeated more than once, and the mean value was recorded. The above investigations were performed in all the enrolled patients independently of the presence of a symptomatic disease.

Severity of spontaneous bleeding was evaluated according to the World Health Organization (WHO) bleeding score: grade 0, no bleeding; grade 1, only cutaneous bleeding; grade 2, mild blood loss; grade 3, gross blood loss, requiring transfusion; grade 4, debilitating blood loss, retinal or cerebral associated with fatality. The history of spontaneous bleeding based on the patients' entire lifetimes. Provoked bleeding episodes were not considered for this study.

Statistical analysis

Data were described as mean and standard deviation (SD) and as counts and percent for continuous and categorical variables, respectively. The association of genotype and phenotype was assessed by means of a generalized linear regression model. The association of the genotype with the clinical outcome during follow-up was evaluated with event-free survival analysis (log-rank test & Cox model). Rate per 100 person year and their 95% confidence intervals (95%CI) were computed, while accounting for familial aggregation. Given the lack of independence of the members of the same families, we adopted the appropriate control for this: for all regression models, Huber-White robust standard errors were computed to account for intra-familial aggregation of data. Observation started at birth. Stata 12.1 (Stata Corp, College Station, TX, USA) was used for computation. A 2-sided p-value<0.05 was considered statistically significant. Post-hoc comparisons need to be interpreted with caution in the framework of multiple tests. Within each phenotype,

tests were performed hierarchically with the increase of the genetical detail and subsequent *p* values were considered at their face 5% value only if the preceding test was significant at the 5% level. Moreover, Bonferroni correction was applied for all multiple and post-hoc comparisons.

RESULTS

Enrollment and mutational screening

A total of 255 consecutive patients belonging to 121 unrelated *MYH9*-RD pedigrees were enrolled. Patients were 134 males and 121 females, and their mean age was 33 years (SD 21). Mutational screening of *MYH9* allowed us to identify 34 different mutations (Table 1). All the variations have been already described as causative of the *MYH9*-RD [Balduini et al., 2011; De Rocco et al., 2013].

In 34 families (28%) mutations affected the HD of NMMHC-IIA. They were missense variations resulting in single amino acid substitutions that were mainly located in two specific regions of the globular head (**Supp. Figure S2**). In 24 families (20% of all families) mutations affected the R702 residue located in the short SH1 helix of the lower 50kDa subdomain [Eddinger and Meer, 2007]. Nine families had mutations of exon 2 hitting residues W33 or V34 of the SH3-like motif, or residues N93, A95 or S96 of the upper 50kDa subdomain [Sellers, 2000]. By investigation of a three-dimensional model of the human NMMHC-IIA head, it was previously demonstrated that all these five residues are clustered together to form a distinct hydrophobic interface between the SH3-like motif and the motor domain [Dominguez et al., 1998; Kahr et al., 2009]. Thus, we referred to these substitutions as mutations of the SH3-like motif/motor domain (SH3/MD) interface. The p.R718W identified in one family was located in the converter subdomain and therefore was the only HD mutation outside the SH1 helix or the SH3/MD interface.

In 87 families (72%) mutations affected the TD. In most cases (n=54, 45%), they were single residue substitutions located in the coiled-coil region. Consistent with data from literature, three residues were most frequently affected: R1165, D1424, and E1841 (8%, 16%, and 12% of families and 9%, 21%, and 13% of patients, respectively) (in bold in Table 1). In 28 families (23%), we identified nonsense or frameshift alterations of exon 41 resulting in deletion of a variable portion of the NHT. The most frequent NHT

alteration was the p.R1933* (20 families, 16%, and 44 patients, 17%). Finally, in rare cases (5 families), we found in-frame deletions or duplications resulting in in-frame alterations affecting the N-terminal part of the coiled-coil (Table 1). The spectrum of mutations identified in our case series was very similar, and, therefore, representative of that of the whole of *MYH9*-RD families reported so far [Balduini et al., 2011].

Genotype-phenotype correlations

To search for genotype-phenotype correlations, we performed four different and complementary analyses. (i) First, we grouped patients according to the NMMHC-IIA domain hit by mutations (HD vs. TD), in order to confirm the previous findings [Pecci et al., 2008a]. (ii) Second, we grouped patients according to the specific region of the protein hit by mutations: the substitutions in the SH1 helix (corresponding to R702 substitutions) were compared with the substitutions in the SH3/MD interface, the substitutions in the coiled-coil region, and the deletions hitting the NHT. The in-frame deletions or duplications in the coiled-coil were excluded from this analysis because of their rarity and to make the coiled-coil group more homogeneous. (iii) A third analysis was carried out by clustering patients according to the residue of NMMHC-IIA hit by mutations, and by comparing the five groups with at least 10 evaluable patients: residue R702 vs. R1165 vs. D1424 vs. E1841 vs. R1933 (in bold in Table 1). (iv) Finally, we considered the possibility that substitution of the same residue with different amino acids could have different effects on phenotype. By taking into account only the mutations with at least 10 evaluable patients, the p.R702C substitution was compared with the p.R702H, and the p.D1424H was compared with the p.D1424N (Table 1).

The phenotype of investigated patients is reported in detail in Supp. Tables S1 and S2. To search for genotype-phenotype correlations, each manifestation of the *MYH9*-RD was analyzed separately.

Nephropathy. Sixty-one of 247 evaluable patients (25%) developed the proteinuric nephropathy (mean age of evaluable cases, 33 years). The mean age at onset of nephropathy was 27 years (SD 14), and 72% of patients were diagnosed before the age of 35. Nephropathy occurred in 44 of 118 pedigrees (37%). This picture resulted in an overall rate per 100 person year of 0.77 (95%CI 0.56-1.08).

The results of genotype-phenotype analyses are detailed in Table 2. The comparison between the two NMMHC-IIA domains confirmed that mutations in the HD are associated with higher incidence of nephropathy than TD mutations ($p<0.001$). However, the analysis according to the different regions of NMMHC-IIA hit by mutations disclosed a remarkably different effect of mutations in the two affected regions of the HD. In fact, substitutions in the SH1 helix were associated with a much higher risk of nephropathy than substitutions in the SH3/MD interface (Table 2; HR 11.3, 95%CI 2.2-58.2, $p<0.001$) (**Figure 1**). The risk deriving from SH3/MD interface substitutions was similar to that globally associated with substitutions in the coiled-coil of the TD, while the deletions at NHT correlated with a significantly lower incidence of kidney damage (Table 2 and **Figure 1**). The event-free survival analysis showed that all patients with SH1 helix (R702) substitutions are expected to develop kidney damage before the age of 45 years (**Figure 1**). The analysis according to the five most frequently affected residues confirmed the more severe consequences of the R702 substitutions and the lower risk associated with the deletions at R1933 compared to mutations at each of the three investigated coiled-coil residues (R1165, D1424 or E1841, Table 2). Moreover, the further analyses suggested that different coiled-coil substitutions could have different effects. In particular, the prognostic significance of the D1424 mutations greatly differed according to the amino acid replacing the aspartic acid. In fact, while the p.D1424H mutation was associated with a notable risk of nephropathy (Table 2), none of the 13 patients with the p.D1424N developed this complication ($p=0.005$ in the comparison with D1424H).

Figure 2 shows the results of the exploratory post-hoc analysis comparing the incidence of kidney damage associated with 7 distinct genotypes. These included the substitutions at the two affected regions of the HD and at the three more frequently hit residues of the coiled-coil. NHT deletions were included as a unique group, as our analysis showed no different prognostic significance among these deletions. Accordingly, similar results were obtained by considering the NHT deletions or deletions at R1933 alone (data not shown). On the contrary, the p.D1424H and the p.D1424N were included as distinct genotypes on the basis of their clearly different prognostic behavior. In summary, the R702 substitutions had the most severe effects. Among the other mutations, the p.D1424H was identified as being associated with a relatively high-risk

profile. Post-hoc analysis showed that the incidence of nephropathy associated with the p.D1424H was significantly higher than that of the E1841 substitution or the NHT deletions, with a statistical trend with respect to the SH3/MD interface or R1165 substitutions, most likely due to the low number of observations in the latter groups. Finally, the substitutions at the SH3/MD interface, R1165 or E1841 appeared associated with a low incidence of nephropathy, and the risk of this complication was almost negligible for the NHT deletions and the p.D1424N (**Figure 2**).

Evolution of nephropathy. We then investigated whether, after the onset of the proteinuric nephropathy, the progression of kidney damage to CRF and ESRD was different in patients with different genotypes. After a median follow-up of 36 months (range 1-228), 40 of the 61 patients with nephropathy (66%) developed CRF. The mean age at onset of CRF was 31 years (SD 15). Twenty-six patients (43%) also developed ESRD (median follow-up, 39 months, range 1-540) at a mean age of 30 years (SD 17). The overall rate per 100 person year for the progression to ESRD was 6.79 (95%CI 4.32-9.53).

We compared the progression of kidney damage between patients with SH1 helix (R702) and those with coiled-coil substitutions, since in the other genotype groups only few patients had nephropathy (two patients for SH3/MD interface substitutions and three for NHT deletions, respectively). Table 3 and **Figure 3** show the significantly more severe evolution for patients with SH1 helix (R702) mutations. Of note, the most remarkable difference between the two groups was observed for progression to ESRD, while only a slight, albeit significant, difference was observed for progression to CRF (Table 3). Finally, no differences in progression to CRF or ESRD were observed among patients with different substitutions within the coiled-coil (D1424, R1165, or E1841).

The picture shown in **Figure 3** suggest that, whereas in patients with R702 substitution this *MYH9* mutation is the only determinant of ESRD, in subjects with coiled-coil substitutions additional genetic or environmental factors are required for the progression to ESRD. The screening of all the *MYH9* coding exons was performed in the 9 patients with coiled-coil mutations who developed ESRD, in order to test whether an additional *MYH9* mutation could explain their more severe evolution. We found that one patient with the p.D1424H carried also an *in trans* p.K910Q substitution inherited from the mother (Seri et al., 2003). As the

patient's mother has no signs of *MYH9*-RD at clinical and laboratory evaluation, the p.K910Q is likely to be a non-pathogenetic variant, even if an effect in addition to that of the p.D1424H cannot be definitely excluded. In the remaining 8 patients, no additional *MYH9* mutations was found. On the whole, these results indicate that the severe evolution of nephropathy in these patients is not ascribable to additional *MYH9* mutations.

Sensorineural deafness. Sensorineural deafness was present in 114 of 237 patients who underwent audiometric examination (48%) and in 67 of 116 pedigrees (58%). Ninety percent of patients with altered audiometric examination had a clinically relevant hearing loss. The mean age at onset was 31 years (SD 19). The ages at onset were homogeneously distributed from the first to the sixth decade, as 36% of patients developed the hearing defect before 20 years of age, 33% between 20 and 40, and 31% after 40. The resulting overall rate per 100 person year was 1.71 (95%CI 1.39-2.11).

Genotype-phenotype correlations for sensorineural deafness are detailed in Table 4. As with nephropathy, the SH1 helix substitutions were associated with the highest risk ($p<0.001$), while the deletions in the NHT correlated with a significantly lower risk compared with mutations in the other NMMHC-IIA regions ($p\leq0.001$). The subsequent analyses (according to residues and mutations) disclosed the different prognostic significance of the different substitutions within the coiled-coil. In fact, the D1424 and the R1165 changes were associated with higher risk of deafness than the E1841 substitution. Moreover, as with nephropathy, the p.D1424N was associated with a particularly low incidence of hearing impairment, which was significantly lower than that deriving from the p.D1424H ($p<0.001$, Table 4).

In summary, our analyses allowed us to assess the risk of deafness associated with the 7 genotypes identified above and defined three distinct prognostic groups (**Figure 4**). Patients with SH1 helix (R702) mutations presented higher risk than all the other genotypes: the event-free survival analysis showed that all of these patients are expected to develop the hearing defect before 40 years of age. Patients with SH3/MD interface, p.D1424H and R1165 substitutions presented an intermediate-high risk of developing deafness, whereas the p.D1424N or p.E1841K substitutions and the NHT deletions were associated with the lowest incidence

(**Figure 4**). The post-hoc analysis confirmed the consistency of the definition of these three prognostic groups. In fact, the risk associated with a given genotype was significantly different from that of each genotype assigned to a different prognostic group, while it did not significantly differ from that of the genotypes assigned to the same prognostic group (data not shown).

Cataract. Cataract was observed in 43 of 235 evaluable patients (18%), thus represented the less frequent extra-hematological manifestation of *MYH9*-RD. In most cases (n=31, 72%) it was bilateral. The mean age at onset was 37 years (SD 30) and 4 patients had congenital forms. The overall rate per 100 person year was 0.57 (95%CI 0.41-0.82).

Confirming previous observations [Pecci et al., 2008a], we found that the incidence of cataract was not different between HD and TD mutations (Table 5). The main finding from the more in-depth analyses was that patients with the NHT deletions have a lower risk of developing cataract than those with substitutions in the coiled-coil or SH1 helix. Consistently, patients with deletions at R1933 presented lower risk than patient with D1424 or R702 substitutions (Table 5). Of note, the highest incidence of cataract was recorded for the p.D1424H substitution, even if further data are needed to confirm the more deleterious effect of this mutation compared to the other genotypes (Table 5).

Thrombocytopenia and bleeding diathesis. In *MYH9*-RD, the routine automated platelet counting overestimates the severity of thrombocytopenia, as cell counters fail to recognize the very large platelets of these patients. The actual platelet count (PLTC) can be assessed only by counting upon phase-contrast microscopy [Balduini et al., 2011]. In our case series, the median PLTC measured by cell counters in all the 255 patients was 31 $x10^9$/L (IQR 16-53). Microscopic PLTC was available for 167 patients, and the median value was 70 $x10^9$/L (IQR 40-95). In the same patient population, the median automated PLTC was 26 $x10^9$/L (IQR 13-46). Of note, the microscopic PLTC was within the normal range (153 to 182 $x10^9$/L) in 6 patients (4%).

Supplementary Table 1 summarizes genotype-phenotype correlations for PLTC as assessed by microscopic counting. In brief, patients with HD mutations had more severe thrombocytopenia with respect to those with TD mutations ($p<0.001$). Statistical significance was reached also when each of the HD genotypes was

compared with each of the TD genotypes. In contrast, no significant differences were observed among the different genotypes within the same NMMHC-IIA domain (Supp. Table S3). Similar results were obtained when the automated PLTCs of all the 255 patients were considered (data not shown).

Evaluation of spontaneous bleeding tendency by the WHO bleeding scale was available for 183 patients. Most cases had no bleeding (105 patients, 57%) or WHO grade 1 bleeding (27 patients, 15%). Thirty-five patients (19%) presented grade 2 bleeding and 16 (9%) had grade 3. The bleeding score strongly correlated with PLTCs, as measured by microscopy or cell counters ($p<0.001$ in both cases) (**Supp. Figure S4**). The patients with grade 3 bleeding had a median microscopic PLTC of 38 $x10^9$/L (IQR 25-55) and an automated count of 10 $x10^9$/L (median, IQR 5-17). Consistent with these observations, the genotype-phenotype correlations for bleeding diathesis showed a picture very similar to that observed for PLTC (Supp. Table S4).

DISCUSSION

The vast majority of *MYH9*-RD patients at birth have only platelet macrocytosis and a variable degree of thrombocytopenia; however, their clinical evolution is very different depending on the occurrence of the non-congenital manifestations of the disease. Thus, predicting the natural history of *MYH9*-RD is particularly important for patients' management and genetic counseling. By the systematic analysis of the largest case series ever reported, we demonstrated that *MYH9* genotype is a major determinant of the disease phenotype, and we defined the disease evolution associated with 7 genotypes that, on the whole, account for about 85% of the *MYH9*-RD cases [Balduini et al., 2011]. These findings are recapitulated in Table 6.

The R702 substitutions are associated with the most severe phenotype. The R702 patients present with severe thrombocytopenia (median PLTC in our case series, 27 $x10^9$/L) and all of them are expected to develop the proteinuric nephropathy and deafness by the fourth decade (**Figures 2 and 4**). Moreover, their nephropathy evolves aggressively, with a median time to progression to ESRD of about 5 years from onset of proteinuria (**Figure 3**). By investigating 30 patients (23 families), we observed almost no variability in their clinical course, demonstrating that the R702 genotype has an almost complete penetrance for severe

thrombocytopenia plus early and aggressive nephropathy and deafness. Some drugs, such as ACE-inhibitors or angiotensin receptor blockers, were suggested to be effective in reducing *MYH9*-RD proteinuria and slowing down progression of kidney damage [Pecci et al., 2008b]. The follow-up for occurrence of proteinuria should therefore be particularly close for R702 patients, in order to start treatment as early as possible. Whereas the severe consequences of R702 mutations have been suggested by earlier observations [Pecci et al., 2008a; Han et al., 2010; Sekine et al., 2010], the present study provided several novel genotype-phenotype correlations. Three results seem particularly relevant. (i) The p.D1424H substitution can be distinguished from all the other non-R702 mutations by a relative and absolute high risk to develop the non-congenital manifestations of the disease. Most of the p.D1424H patients are expected to have developed proteinuria by the sixth decade of life (**Figure 2**), and all of them are predicted to develop deafness before the age of 60 (**Figure 4**); moreover, the p.D1424H results in a higher probability of cataract occurrence compared to all the other analyzed genotypes except R702 mutations (Table 4). Thus, in a hierarchical prognostic model, p.D1424H is the genotype associated with the highest risk of a syndromic disease after the R702 mutations. Interestingly, the substitution of the same aspartic acid with asparagine is much less deleterious, since it associated with a significantly lower incidence of all the non-congenital features of the disease. (ii) Except for the mutations at R702, most of the HD mutations reported so far hit residues that are clustered to form a distinct hydrophobic seam at the SH3/MD interface [Kahr et al., 2009; Balduini et al., 2011]. These mutations associated with a less severe phenotype than the R702 substitutions. These results contradict the conclusions from our previous, smaller genotype-phenotype study, which concluded that all patients with HD mutations share the same severe prognosis [Pecci et al., 2008a]. Instead, the SH3/MD substitutions associate with an "auditory" phenotype: all these patients are expected to develop sensorineural deafness before 60 years of age (**Figure 4**), while the risk of developing nephropathy and cataract is low (**Figure 2** and Table 5). The same auditory phenotype is linked to the substitutions at R1165 (Table 6). (iii) Finally, the p.D1424N and p.E1841K substitutions, as well as the mutations hitting the NHT, correlated with a low incidence of the non-congenital complications, and therefore with a high probability that thrombocytopenia remains the only manifestation of the *MYH9*-RD throughout life. In particular, the risk profile deriving from the NHT deletions and from the p.D1424N was found to be particularly low.

The different evolution of proteinuric nephropathy between patients with R702 mutations and those with coiled-coil substitutions is another relevant aspect from a clinical point of view. In fact, while proteinuria is expected to rapidly evolve to ESRD in nearly all patients with R702 mutations, less than half of patients with coiled-coil mutations and proteinuria will progress to ESRD (**Figure 3**). Considering only patients with ESRD, the median age at onset of ESRD was 24 years (SD 9) for R702 and 42 years (SD 23) for coiled-coil mutations, respectively. Therefore, even if certain subjects with coiled-coil mutations frequently develop kidney damage (as with the p.D1424H patients), their defect is less progressive. This picture suggests that, whereas for R702 patients the *MYH9* mutation is the only determinant of ESRD development, for patients with coiled-coil substitutions additional genetic or environmental factors interact with the *MYH9* mutation to determine progression to ESRD. The absence of additional *MYH9* mutations in the patients with coiled-coil substitutions who developed ESRD suggests that variants in other genes interacting with *MYH9* represent the additional genetic factors for their more severe evolution.

It is important to underline that this study was aimed at investigating the clinical evolution of the typical *MYH9*-RD, which is defined by congenital macrothrombocytopenia and NMMHC-IIA leukocyte inclusions, and represents the markedly most frequent known phenotype deriving from *MYH9* mutations. However, the p.R705H mutation of NMMHC-IIA was reported as responsible for DFNA17, a non-syndromic form of deafness, in two unrelated pedigrees [Lalwani et al., 2000]. Patients having further possible phenotypes not including thrombocytopenia or leukocyte NMMHC-IIA inclusions would be missed by the protocol used for recruitment to this study. Future investigation is required to explore the possibility that some *MYH9* variations could result in further syndromic or non-syndromic phenotypes other than *MYH9*-RD or DFNA17.

It is generally accepted that the more severe consequences of the HD vs. TD mutations derive from the fact that the HD mutants impair the NMM-IIA ATPase activity, while the TD alterations impact molecule assembly but do not affect ATPase activity [Balduini et al., 2011]. However, the present study identified some relevant exceptions to this scheme based on simple HD vs. TD contraposition, as the R702 mutations have worse effects than the SH3/MD substitutions, and the TD p.D1424H mutation showed the most

deleterious effect among the non-R702 alterations. This suggests that, at least for some mutants, additional pathogenetic mechanisms are involved in alteration of NMM-IIA function.

Consideration of the molecular interactions within the myosin head allows us to propose a testable hypothesis for the basis of the differences between MD/SH3 interface and R702 mutations. Hu and colleagues reported that both the p.N93K (in the SH3/MD interface) and the p.R702C (SH1 helix) greatly reduce the ATPase activity of NMM-IIA, and that the extent of the reduction was even greater for the p.N93K [Hu et al., 2002]. Thus, it seems hard to explain the more severe consequences on phenotype of the R702 compared to the SH3/MD substitutions just on the basis of defective ATPase activity. However, by homology with known crystal structures of other myosin IIs, the R702 interacts directly with the relay loop near D503, which is the vital conduit between ATP hydrolysis and the position of the converter and thus of the lever swing [Dominguez et al., 1998; Bauer et al., 2000; Gourinath et al., 2003; Risal et al., 2004]. In particular, R702 stabilizes the link between the SH1 helix and the relay loop by its long paraffin chain contributing to the hydrophobic seam between these two key regions and also likely forming a salt bridge with the D507 in the loop. Mutation to the shorter side chains of cysteine, histidine, or serine with their reduced hydrophobic character will weaken the seam and disrupt the salt bridge. By consequence, the coupling between the motor and converter domains will be weakened, thus uncoupling ATPase activity from force production. In contrast, mutations in the SH3/MD interface, as the linkage to the relay loop is indirect, have the potential to affect ATPase activity through different routes, including an overall destabilisation of HD folding. Consistent with this, Hu and colleagues reported greater aggregation *in vitro* of the N93K than for the R702C [Hu et al., 2002]. Thus, a hypothesis for the greater severity of R702 mutations than SH3/MD interface mutations in *MYH9*-RD is that the former could be defective in both ATPase activity and holding tension whereas the latter has low ATPase but could maintain tension.

Possible molecular mechanisms for the impact of D1424 mutations are worthy of discussion because this can suggest why different mutations at this residue can have very different impacts, and can further suggest future biophysical experiments on expressed proteins. In general, the mechanism of TD point mutations will depend on the position of the residue within the heptad repeat motif (*abcdefg*) of amino acid residues that is

the building block of the coiled-coil tail (**Suppl. Figure S1**, **D**) [Franke et al., 2005]. Any given TD mutant could either enhance or reduce any or all of: (i) coiled-coil stability, (ii) filament nucleation and assembly, (iii) folding of the molecule into the 10S inactive conformation (**Supp. Figure S1**, **A-C**). Indeed, this third alternative has not been considered in previous work, but could be germane because in 10S the tail is folded into three roughly equal and closely apposed segments that wrap around one of the heads [Burgess et al., 2007]. D1424 occupies a heptad *c* position in the NMMHC-IIA tail. Mutation is thus unlikely to perturb the helical stability or interactions between the two chains of the molecule (the hydrophobic seam here is well populated by hydrophobic residues and therefore stable). The p.D1424H is a negative to positive charge change and is thus expected to alter ionic interactions more than p.D1424N, which is a negative to polar/uncharged change. The charge change in p.D1424H could have a destabilizing impact on packing of molecules into functional filaments by weakening interactions with positive-charged zones of adjacent molecules. However, we propose that an additional impact might be on the stability of the 10S, inactive conformer. In fact, D1424's position in the tail, about 88 nm from the heads, corresponds to where the second segment of the folded tail contacts the motor domain, close to the converter subdomain in a region of net positive surface charge (**Supp. Figure S1, A**) [Burgess et al., 2007; Jung et al., 2008]. Since this compact conformer is sensitive to salt, the stabilizing interactions are likely ionic, so the negative to positive charge change in p.D1424H could be much more destabilizing than the p.D1424N, causing the molecules to unfold. NMMHC-IIA unfolding would favor filament formation, and thus might make this mutant more sensitive to activation and prolong activity following dephosphorylation of the regulatory light chains. Perturbations of monomer-polymer equilibria could underlie the increased association of mutant NMM-IIA with the actin cytoskeleton that was experimentally observed in *MYH9*-RD platelets [Canobbio et al., 2005]. Interestingly, the R1165 mutations, which are also associated with a significant incidence of extra-hematological manifestations, are also located in a potentially critical region for the stability of the 10S conformer. Measurements of the lengths of the three segments of the tail in smooth muscle myosin suggest that the first sharp bend of the 10S conformer is at residue 1175, which would be S1163 in NMMHC-IIA (**Supp. Figure S1, A**) [Eddinger and Meer, 2007]. The R1165 may therefore be a part of this bend, or if it just follows the bend could be interacting with the adjacent first segment of folded tail, and mutations could destabilize the 10S soluble shutdown state.

In conclusion, this study identified novel genotype-phenotype correlations that allow us to predict the clinical evolution of *MYH9*-RD in about 85% of patients. These data are essential for patients' clinical management and genetic counseling, but are also useful for the elucidation of molecular pathogenesis of the disease.

ACKNOWLEDGEMENTS

This work was supported by a grant from IRCCS Policlinico San Matteo Foundation (A.P.); by the grant 34/07 of IRCCS Burlo Garofolo (A.S.); by the Wellcome Trust [094231] (K.J.D.L. and P.J.K.).
The authors have no conflict of interest to declare.

REFERENCES

Althaus K, Greinacher A. 2009. MYH9-related platelet disorders. Semin Thromb Hemost 35:189-203.

Althaus K, Greinacher A. 2010. MYH-9 Related Platelet Disorders: Strategies for Management and Diagnosis. Transfus Med Hemother 37:260-267.

Arrondel C, Vodovar N, Knebelmann B, Grünfeld JP, Gubler MC, Antignac C, Heidet L. 2002. Expression of the nonmuscle myosin heavy chain IIA in the human kidney and screening for MYH9 mutations in Epstein and Fechtner syndromes. J Am Soc Nephrol 2002;13:65-74.

Balduini CL, Pecci A, Savoia A. 2011. Recent advances in the understanding and management of *MYH9*-related inherited thrombocytopenias. Br J Haematol 154:161-174.

Bauer CB, Holden HM, Thoden JB, Smith R, Rayment I. 2000. X-ray structures of the apo and MgATP-bound states of Dictyostelium discoideum myosin motor domain. J Biol Chem 275:38494-38499.

Baumketner A. 2012. The mechanism of the converter domain rotation in the recovery stroke of myosin motor protein. Proteins 80:2701-2710.

Burgess SA, Yu S, Walker ML, Hawkins RJ, Chalovich JM, Knight PJ. 2007. Structures of smooth muscle myosin and heavy meromyosin in the folded, shutdown state. J Mol Biol 372:1165-1178.

Canobbio I, Noris P, Pecci A, Balduini A, Balduini CL, Torti M. 2005. Altered cytoskeleton organization in platelets from patients with MYH9-related disease. J Thromb Haemost 3:1026-1035

De Rocco D, Heller PG, Girotto G, Pastore A, Glembotsky AC, Marta RF, Bozzi V, Pecci A, Molinas FC, Savoia A. 2009. MYH9 related disease: a novel missense Ala95Asp mutation of the MYH9 gene. Platelets 20:598-602.

De Rocco D, Zieger B, Platokouki H, Heller PG, Pastore A, Bottega R, Noris P, Barozzi S, Glembotsky AC, Pergantou H, Balduini CL, Savoia A, et al. 2013. MYH9-related disease: five novel mutations expanding the spectrum of causative mutations and confirming genotype/phenotype correlations. Eur J Med Genet 56:7-12.

Dominguez R, Freyzon Y, Trybus KM, Cohen C. 1998. Crystal structure of a vertebrate smooth muscle myosin motor domain and its complex with the essential light chain: visualization of the pre-power stroke state. Cell 94:559-571.

Dong F, Li S, Pujol-Moix N, Luban NL, Shin SW, Seo JH, Ruiz-Saez A, Demeter J, Langdon S, Kelley MJ. 2005. Genotype-phenotype correlation in MYH9-related thrombocytopenia. Br J Haematol 130:620-627.

Eddinger TJ, Meer DP. 2007. Myosin II isoforms in smooth muscle: heterogeneity and function. Am J Physiol Cell Physiol 293:C493-508.

Franke JD, Dong F, Rickoll WL, Kelley MJ, Kiehart DP. 2005. Rod mutations associated with MYH9-related disorders disrupt nonmuscle myosin-IIA assembly. Blood 105:161-169.

Gourinath S, Himmel DM, Brown JH, Reshetnikova L, Szent-Györgyi AG, Cohen C. 2003. Crystal structure of scallop Myosin s1 in the pre-power stroke state to 2.6 a resolution: flexibility and function in the head. Structure 11:1621-1627.

Han KH, Lee H, Kang HG, Moon KC, Lee JH, Park YS, Ha IS, Ahn HS, Choi Y, Cheong HI. 2011. Renal manifestations of patients with MYH9-related disorders. Pediatr Nephrol 26:549-555.

Heath KE, Campos-Barros A, Toren A, Rozenfeld-Granot G, Carlsson LE, Savige J, Denison JC, Gregory MC, White JG, Barker DF, Greinacher A, Epstein CJ, et al. 2001. Nonmuscle myosin heavy chain IIA mutations define a spectrum of autosomal dominant macrothrombocytopenias: May-Hegglin anomaly and Fechtner, Sebastian, Epstein, and Alport-like syndromes. Am J Hum Genet 69:1033-1045.

Hu A, Wang F, Sellers J R. 2002. Mutations in human nonmuscle myosin 2A found in patients with May-Hegglin anomaly and Fechtner syndrome result in impaired enzymatic function. J Biol Chem 277:46512-46517.

Jang MJ, Park HJ, Chong SY, Huh JY, Kim IH, Jang JH, Kim HJ, Oh D. 2012. A Trp33Arg mutation at exon 1 of the MYH9 gene in a Korean patient with May-Hegglin anomaly. Yonsei Med J 53:662-666.

Jung HS, Komatsu S, Ikebe M, Craig R. 2008. Head-head and head-tail interaction: a general mechanism for switching off myosin II activity in cells. Mol Biol Cell 19:3234-3242.

Kahr WH, Savoia A, Pluthero FG, Li L, Christensen H, De Rocco D, Traivaree C, Butchart SE, Curtin J, Stollar EJ, Forman-Kay JD, Blanchette VS. 2009. Megakaryocyte and platelet abnormalities in a patient with a W33C mutation in the conserved SH3-like domain of myosin heavy chain IIA. Thromb Haemost 102:1241-1250.

Kelley MJ, Jawien W, Ortel TL, Korczak JF. 2000. Mutation of MYH9, encoding non-muscle myosin heavy chain A, in May-Hegglin anomaly. Nat Genet 26:106-108.

Kunishima S, Kojima T, Matsushita T, Tanaka T, Tsurusawa M, Furukawa Y, Nakamura Y, Okamura T, Amemiya N, Nakayama T, Kamiya T, Saito H. 2001. Mutations in the NMMHC-A gene cause autosomal dominant macrothrombocytopenia with leukocyte inclusions (May-Hegglin anomaly/Sebastian syndrome). Blood 97:1147-1149.

Kunishima S, Matsushita T, Kojima T, Sako M, Kimura F, Jo EK, Inoue C, Kamiya T, Saito H. 2003. Immunofluorescence analysis of neutrophil nonmuscle myosin heavy chain-A in MYH9 disorders: association of subcellular localization with MYH9 mutations. Lab Invest 83:115-122.

Kunishima S, Saito H. 2010. Advances in the understanding of MYH9 disorders. Curr Opin Hematol 17:405-410.

Lalwani AK, Goldstein JA, Kelley MJ, Luxford W, Castelein CM, Mhatre AN. 2000. Human nonsyndromic hereditary deafness DFNA17 is due to a mutation in nonmuscle myosin MYH9. Am J Hum Genet 67:1121-1128.

Levey AS, Stevens LA, Schmid CH, Zhang YL, Castro AF 3rd, Feldman HI, Kusek JW, Eggers P, Van Lente F, Greene T, Coresh J; CKD-EPI (Chronic Kidney Disease Epidemiology Collaboration). 2009. A new equation to estimate glomerular filtration rate. Ann Intern Med 150:604-612.

Pecci A, Panza E, Pujol-Moix N, Klersy C, Di Bari F, Bozzi V, Gresele P, Lethagen S, Fabris F, Dufour C, Granata A, Doubek M, et al. 2008a. Position of nonmuscle myosin heavy chain IIA (NMMHC-IIA) mutations predicts the natural history of *MYH9*-related disease. Hum Mutat 29:409-417.

Pecci A, Granata A, Fiore CE, Balduini CL. 2008b. Renin-angiotensin system blockade is effective in reducing proteinuria of patients with progressive nephropathy caused by MYH9 mutations (Fechtner-Epstein syndrome). Nephrol Dial Transplant 23:2690-2692.

Pecci A, Panza E, De Rocco D, Pujol-Moix N, Girotto G, Podda L, Paparo C, Bozzi V, Pastore A, Balduini CL, Seri M, Savoia A. 2010. *MYH9* related disease: four novel mutations of the tail domain of myosin-9 correlating with a mild clinical phenotype. Eur J Haematol 84:291-297.

Risal D, Gourinath S, Himmel DM, Szent-Györgyi AG, Cohen C. 2004. Myosin subfragment 1 structures reveal a partially bound nucleotide and a complex salt bridge that helps couple nucleotide and actin binding. Proc Natl Acad Sci USA 101:8930-8935.

Sanborn KB, Mace EM, Rak GD, Difeo A, Martignetti JA, Pecci A, Bussel JB, Favier R, Orange JS. 2011. Phosphorylation of the myosin IIA tailpiece regulates single myosin IIA molecule association with lytic granules to promote NK-cell cytotoxicity. Blood 118:5862-5871.

Savoia A, De Rocco D, Panza E, Bozzi V, Scandellari R, Loffredo G, Mumford A, Heller PG, Noris P, De Groot MR, Giani M, Freddi P, et al. Heavy chain myosin 9-related disease (MYH9 -RD): neutrophil inclusions of myosin-9 as a pathognomonic sign of the disorder. Thromb Haemost 103:826-832.

Sekine T, Konno M, Sasaki S, Moritani S, Miura T, Wong WS, Nishio H, Nishiguchi T, Ohuchi MY, Tsuchiya S, Matsuyama T, Kanegane H, et al. 2010. Patients with Epstein-Fechtner syndromes owing to MYH9 R702 mutations develop progressive proteinuric renal disease. Kidney Int 78:207-214.

Sellers JR. 2000. Myosins: a diverse superfamily. Biochim Byoph Acta 1496:3-22.

Seri M, Cusano R, Gangarossa S, Caridi G, Bordo D, Lo Nigro C, Ghiggeri GM, Ravazzolo R, Savino M, Del Vecchio M, d'Apolito M, Iolascon A, et al. 2000. Mutations in MYH9 result in the May-Hegglin anomaly, and Fechtner and Sebastian syndromes. The May-Hegglin/Fechtner Syndrome Consortium. Nat Genet 26:103-105.

Seri M, Pecci A, Di Bari F, Cusano R, Savino M, Panza E, Nigro A, Noris P,Gangarossa S, Rocca B, Gresele P, Bizzaro N, et al. 2003. MYH9-related disease: May-Hegglin anomaly, Sebastian syndrome, Fechtner syndrome, and Epstein syndrome are not distinct entities but represent a variable expression of a single illness. Medicine (Baltimore) 82:203-215.

Sweeney HL, Houdusse A. 2010. Structural and functional insights into the Myosin motor mechanism. Annu Rev Biophys 39:539-557.

Vicente-Manzanares M, Ma X, Adelstein RS, Horwitz AR. 2009. Non-muscle myosin II takes centre stage in cell adhesion and migration. Nat Rev Mol Cell Biol 10:778-790.

FIGURE LEGENDS

Figure 1. Occurrence of nephropathy according to the region of NMMHC-IIA affected by mutation. The association of genotype with the occurrence of nephropathy was assessed over time by means of event-free survival analysis. Patient's age was used to measure time. The follow-up was stopped at the age of diagnosis of nephropathy or at the last phenotype evaluation in the case of censoring. Only p values ≤ 0.05 are reported. After Bonferroni correction, significance for $p \leq 0.008$.

Figure 2. Evolution of nephropathy to ESRD in patients with SH1 helix (R702)substitutions or coiled-coil substitutions. The follow-up was initiated at the time of diagnosis of nephropathy and stopped at the time of diagnosis of ESRD or at the last phenotype evaluation in the case of censoring.

Figure 3. Occurrence of nephropathy in patients with different MYH9 mutations. The figure shows the results of the post-hoc statistical comparison between 7 different *MYH9* genotypes. Genotypes were identified by comparing patients with mutations in four different regions of the NMMHC-IIA, then patients with mutations at the five most frequently hit residues of these regions. A further analysis compared the patients with p.R702C with those with the p.R702H, and the patients with p.D1424H with those carrying the p.D1424N. On the whole, the characterized genotypes are responsible for about 85% of the reported *MYH9*-RD cases. Only p values ≤ 0.05 are reported. After Bonferroni correction, significance for $p \leq 0.002$ for all the new comparisons. **[1]** = significance for $p \leq 0.008$ and **[2]** = significance for $p \leq 0.005$ after Bonferroni correction (see notes to Table 2).

Figure 4. Occurrence of sensorineural deafness in patients with different MYH9 mutations. Figure shows the results of the post-hoc statistical comparison between 7 different genotypes. Only p values ≤ 0.05 are reported. After Bonferroni correction, significance for $p \leq 0.002$ for all the new comparisons. **[1]** = significance for $p \leq 0.008$ and **[2]** = significance for $p \leq 0.005$ after Bonferroni correction (see notes to Table 4).

Supporting Figure S1. Schematic representation of non-muscle myosin IIA (NMM-IIA) domain structure, folding and assembly. (**A**): Diagram of the folded, shut-down 10S conformation of NMM-IIA based on the structure of smooth muscle myosin as seen by negative stain EM (adapted from Burgess et al. 2007). The tail folds into three segments of approximately equal length (numbered 1, 2 and 3). The amino acid residue numbers for the bends are derived assuming homology with smooth muscle myosin. The position of D1424 is indicated (red dot) on tail segment 2: it lies adjacent to the converter subdomain (yellow) of the left head. The R1165 (green dot) is located in a region where the tail forms a sharp bend between segment 1 and 2 in the 10S conformation. Phosphorylation of the regulatory light chain (RLC) causes unfolding of NMM-IIA into the 6S conformation. (**B**): Domain structure of 6S NMM-IIA. The essential light chain (ELC; green) and RLC (orange) bind to the lever arm region of the heavy chain. Two NMM-IIA heavy chains dimerise through their long, C-terminal α-helices to form a coiled-coil tail with a non-helical tail piece at the C-terminus starting at G1924. (**C**): Interactions between the tails of 6S NMM-IIA molecules yield bipolar filaments that function to draw together actin filaments of opposite polarity. (**D**) Heptad plot showing hydrophobic and ionic interactions in the coiled-coil. The sequence is plotted as a helical wheel in which each helix is modified to 3.5 residues per turn such that two turns coincide with one heptad repeat. The resulting paired structure is viewed along the helix axis. Hydrophobic residues in the 'a' and 'd' positions can escape interaction with aqueous solution by forming a hydrophobic seam when the two polypeptide chains associate together (solid arrows). The 'g' and 'e' residues are often charged and can make ionic 'g' to 'e' interactions (shown by the dotted arrows) across the seam, which stabilizes the coiled-coil.

Supporting Figure S2. Schematic representation of the three-dimensional structure of the NMMHC-IIA head domain (HD). The globular head includes four subdomains: from the N- to the C-terminus, they are the SH3-like motif, the upper and the lower 50kDa subdomains, and the converter subdomain. The two 50 kDa subdomains form the so-called motor domain, as it contains the functional regions essential for production of chemomechanical forces. The converter domain connects the lever arm that amplifies the movement produced by conformational changes of the motor domain. In our case series, the HD mutations were mostly located in two specific regions of the head: a distinct hydrophobic interface between the N-terminal SH3 motif and the 50kDa upper subdomain (SH3/MD interface, blue dot) (Kahr et al., 2009;

Dominguez et al. 1998) and at R702 (red dot) localized in the SH1 helix (yellow) of the 50kDa lower subdomain. The relay loop is also schematically represented (see text).

Supporting Figure S3. Enrollment to this genotype-phenotype study. Patients having the inclusion criteria were identified at the different centers participating in the network of the Italian registry for *MYH9*-RD, whereas the immunofluorescence assay for NMMHC-IIA and molecular screening of *MYH9* were centralized, as detailed in the text.

Supporting Figure S4. Correlation between microscopic platelet count and WHO bleeding score. For each WHO bleeding grade, median platelet count (midline), 25^{th}-75^{th} percentiles (box) and extremes (whiskers) are shown.

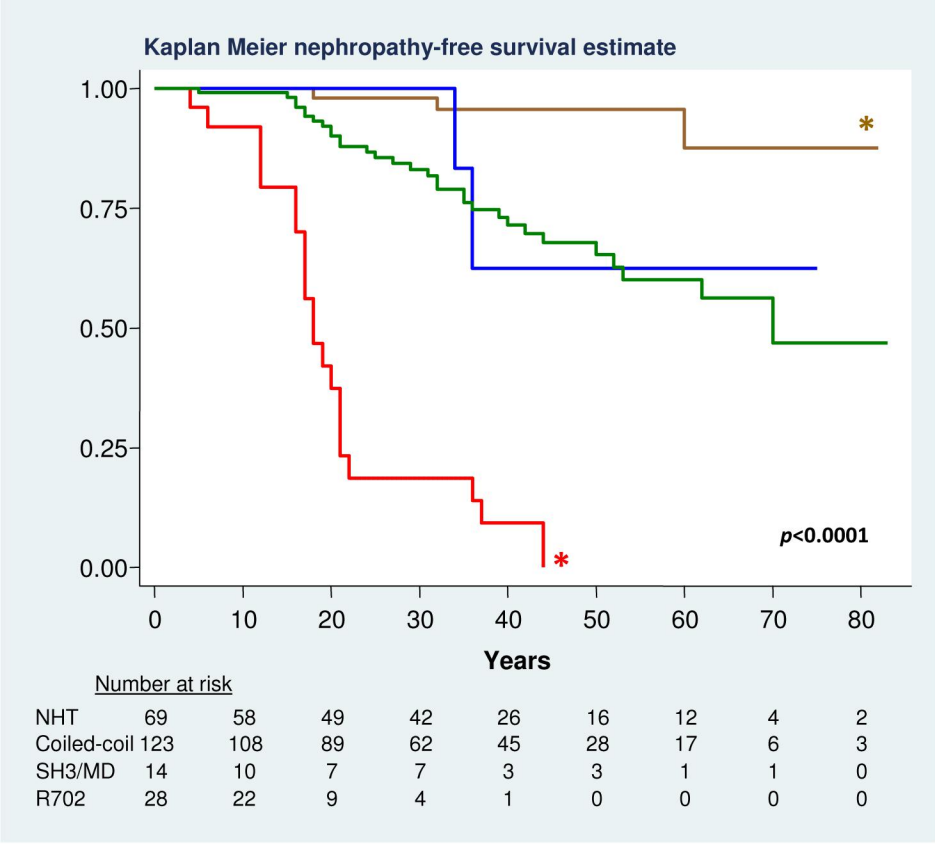
Kaplan Meier nephropathy-free survival estimate
1.00
0.75
0.50
0.25
0.00
0
10
20
30
40
50
60
70
80
Years
p<0.0001
*
*
Number at risk
NHT 69 58 49 42 26 16 12 4 2
Coiled-coil 123 108 89 62 45 28 17 6 3
SH3/MD 14 10 7 7 3 3 1 1 0
R702 28 22 9 4 1 0 0 0 0
SH3/MD interface
SH1 helix (R702)
Coiled-coil
NHT
* p<0.001 vs all the other groups
* p<0.001 vs. coiled-coil <0.05 vs. SH3/MD

Figure 1

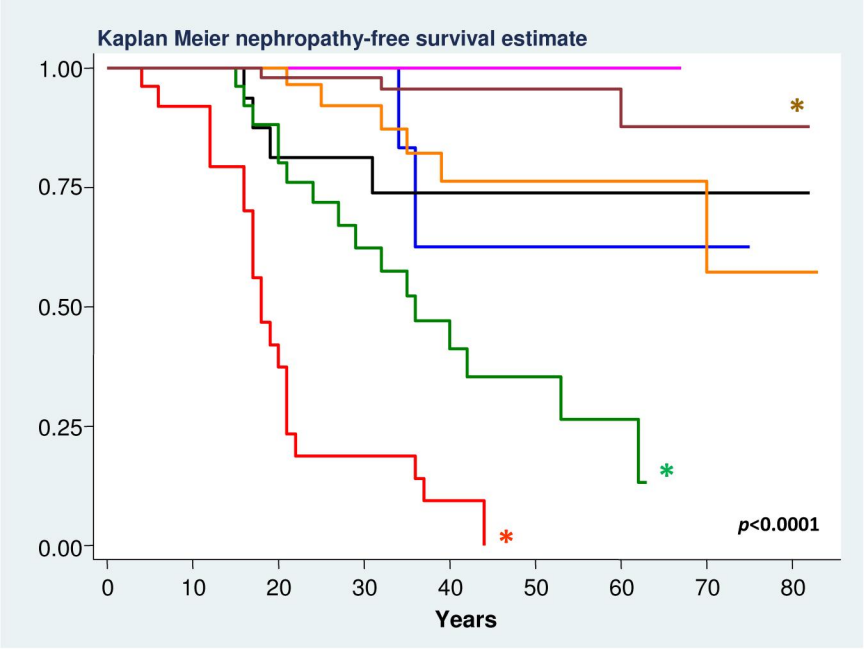
Kaplan Meier nephropathy-free survival estimate
1.00
0.75
0.50
0.25
0.00
0
10
20
30
40
50
60
70
80
Years
p<0.0001
*
*
*
SH3/MD interface
R702 (SH1 helix)
R1165
D1424H
D1424N
E1841
NHT
* p<0.001 vs all the other groups
* p<0.0001 vs. NHT <0.001 vs. E1841, 0.005 vs. D1424N [2], 0.03 vs. R1165
* p=0.04 vs. SH3/MD [1], 0.02 vs. R1165, 0.05 vs. E1841

Figure 2

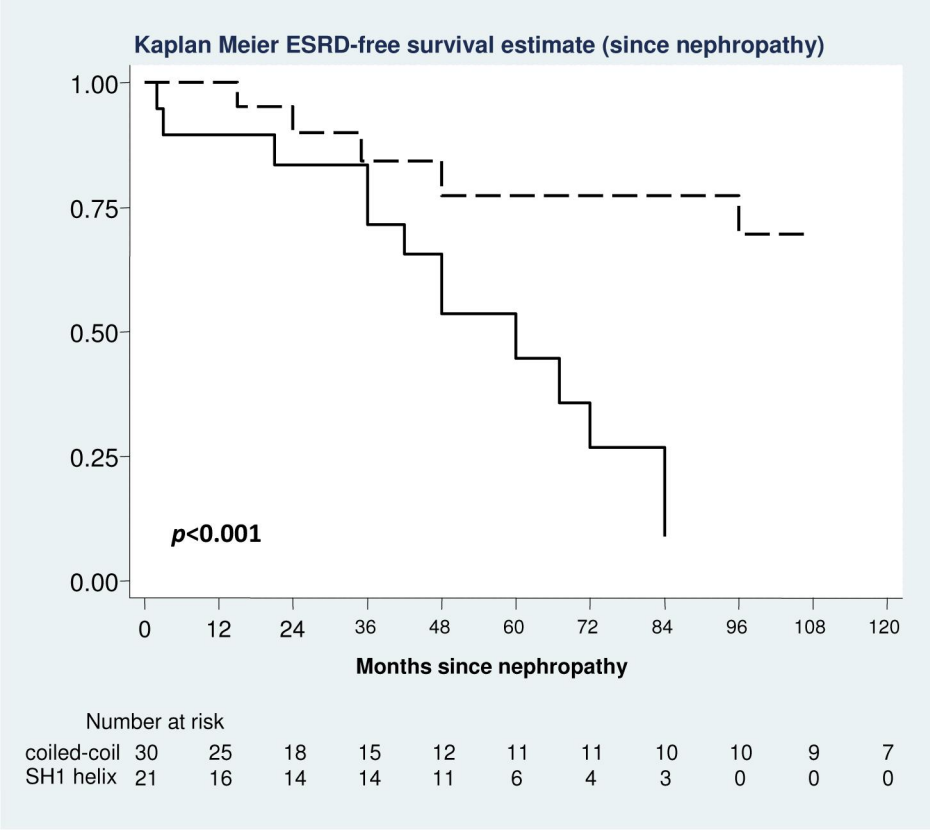
Kaplan Meier ESRD-free survival estimate (since nephropathy)
1.00
0.75
0.50
0.25
0.00
p<0.001
0
12
24
36
48
60
72
84
96
108
120
Months since nephropathy
Number at risk
coiled-coil 30 25 18 15 12 11 11 10 10 9 7
SH1 helix 21 16 14 14 11 6 4 3 0 0 0
SH1 helix (R702)
Coiled-coil

Figure 3

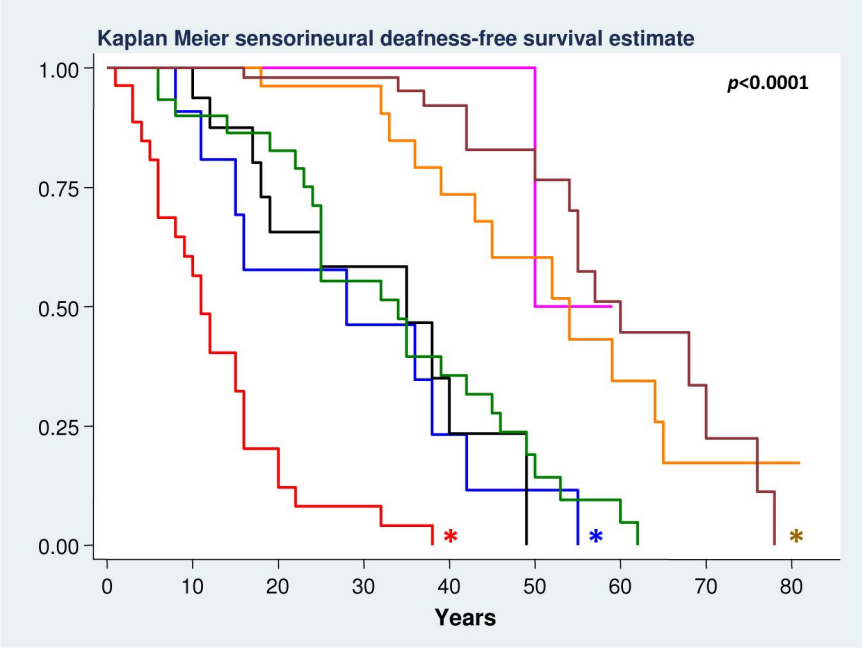
Kaplan Meier sensorineural deafness-free survival estimate
p<0.0001
1.00
0.75
0.50
0.25
0.00
0
10
20
30
40
50
60
70
80
Years
SH3/MD interface
R702 (SH1 helix)
R1165
D1424H
D1424N
E1841
NHT
* p<0.001 vs all the other groups
* p<0.0001 vs. NHT [1] <0.001 vs. E1841, 0.004 vs. D1424N [2]
* p<0.0001 vs. R1165 and SH3/MD [1]

Figure 4

Table 1. Results of mutational screening in 255 *MYH9*-RD patients (121 families).

					N. of patients (n. of families)		
Exon	**Nucleotide change**	**NMMHC-IIA domain**	**NMMHC-IIA region**	**Amino acid change**	**Total enrolled**	**Previously reported**	**Ref.**
2	c.99G>T	HD	SH3/MD i	p.W33C	1 (1)	1 (1)	A
2	c.101T>G	HD	SH3/MD i	p.V34G	3 (1)	3 (1)	D
2	c.279C>G	HD	SH3/MD i	p.N93K	1 (1)	1 (1)	B
2	c.284C>A	HD	SH3/MD i	p.A95D	3 (1)	1 (1)	G
2	c.287C>T	HD	SH3/MD i	p.S96L	6 (5)	3 (3)	B,G
17	c.2104C>T	HD	SH1 helix	**p.R702C**	**19 (17)**	15 (14)	B,G
17	c.2104C>A	HD	SH1 helix	**p.R702S**	**1 (1)**	1(1)	D
17	c.2105G>A	HD	SH1 helix	**p.R702H**	**11 (6)**	7(4)	B,G
17	c.2152C>T	HD	Converter	p.R718W	1 (1)	1 (1)	B
21	c.2539 _2559dup	TD	Coiled-coil	p.M847_ E853dup	2 (1)	2 (1)	D
25	c.3142 _3162del	TD	Coiled-coil	p.K1048_ E1054del	2 (1)	2 (1)	D
25	c.3195 _3215del	TD	Coiled-coil	p.E1066_ A1072del	3 (2)	1 (1)	B
25	c.3195 _3215dup	TD	Coiled-coil	p.E1066_ A1072dup	3 (1)	3 (1)	G
26	c.3463A>G	TD	Coiled-coil	p.T1155A	1 (1)	1 (1)	G
26	c.3464C>T	TD	Coiled-coil	p.T1155I	4 (1)	2 (1)	B
26	c.3485G>C	TD	Coiled-coil	p.R1162T	3 (2)	3 (2)	C
27	c.3493C>T	TD	Coiled-coil	**p.R1165C**	**18 (8)**	8 (3)	B
27	c.3494G>T	TD	Coiled-coil	**p.R1165L**	**5 (2)**	1 (1)	G

31	c.4270G>C	TD	Coiled-coil	**p.D1424H**	**33 (9)**	20 (5)	B,G
31	c.4270G>A	TD	Coiled-coil	**p.D1424N**	**13 (8)**	7 (6)	B,G
31	c.4270G>T	TD	Coiled-coil	**p.D1424Y**	**7 (3)**	2 (2)	B,G
31	c.4339G>T	TD	Coiled-coil	p.D1447Y	1 (1)	1 (1)	D
31	c.4340A>T	TD	Coiled-coil	p.D1447V	5 (2)	4 (1)	B
32	c.4546G>A	TD	Coiled-coil	p.V1516M	3 (1)	2 (1)	E
33	c.4670G>T	TD	Coiled-coil	p.R1557L	2 (1)	2 (1)	E
39	c.5521G>A	TD	Coiled-coil	**p.E1841K**	**34 (15)**	24 (11)	B,G
41	c.5770 _5779del	TD	NHT	p.G1924Rfs*21	3 (1)	3 (1)	E
41	c.5773delG	TD	NHT	p.D1925Tfs*23	5 (1)	4 (1)	B
41	c.5788delG	TD	NHT	p.V1930Cfs*18	4 (1)	1 (1)	E
41	c.5797C>T	TD	NHT	**p.R1933***	**44 (20)**	20 (13)	B,G
41	c.5797delC	TD	NHT	p.R1933Efs*15	2 (1)	2 (1)	B
41	c.5800delA	TD	NHT	p.M1934Wfs*14	2 (1)	2 (1)	F
41	c.5821delG	TD	NHT	p.D1941Mfs*7	5 (2)	5 (2)	B
41	c.5833G>T	TD	NHT	p.E1945*	5 (1)	3 (1)	B

Notes: the **five residues** most frequently affected by mutations (see text) are evidenced in **bold**. Nucleotide numbering reflects the MYH9 cDNA with +1 corresponding to the A of the ATG translation initiation codon in the reference sequence (RefSeq NM_002473.4). The initiation codon is codon 1. All the mutations are enlisted in a locus specific mutation database (http://www.LOVD.nl/MYH9) at the Leiden Open Variation Database.

Abbreviations: HD = Head Domain; TD = Tail Domain; SH3/MD i = SH3-like motif/motor domain interface; NHT = Non-Helical Tailpiece. Ref.= reference.

References: A = Kahr et al., 2009 (reference listed in the text). B = Pecci et al., 2008a (reference listed in the text). C = Vettore S et al., Eur J Med Genet 2010; 53: 256-60. D = De Rocco D et al., 2013 (reference listed in the text). E = Pecci A et al., 2010 (reference listed in the text). F = Savoia A et al., Ann Hematol 2010; 89:1057-9. G = Savoia A et al., 2010 (reference listed in the text).

Table 2 - Correlations between genotype and incidence of nephropathy in 247 *MYH9*-RD patients.

	N. of patients (families)	Affected patients, %	Mean age at onset, years (SD)	**Rate per 100 person year (95% CI)**	***p* values**
NMMHC-IIA domain					
Head	45 (33)	26 (58%)	20 (10)	**2.73 (1.63-4.41)**	$p<0.001$
Tail	202 (85)	35 (17%)	32 (15)	**0.52 (0.33-0.86)**	
NMMHC-IIA region					$p<0.001$
SH3/MD interface	14 (9)	2 (14%)	35 (1)	**0.52 (0.10-4.02)**	
SH1 helix (R702)	30 (23)	23 (77%)	19 (10)	**4.35 (3.29-5.65)**	$p<0.001$ vs. all other groups [1]
Coiled-coil	123 (53)	31 (25%)	31 (15)	**0.75 (0.47-1.27)**	
NHT	69 (27)	3 (4%)	37 (21)	**0.12 (0.02-1.72)**	$p<0.001$ vs. coiled-coil, $p<0.05$ vs. SH3/MD interface [1]
NMMHC-IIA residue					$p<0.001$
R 702	30 (23)	23 (77%)	19 (10)	**4.35 (3.29-5.65)**	$p<0.001$ vs. all other groups [2]
R 1165	21 (10)	4 (19%)	21 (7)	**0.57 (0.08-1.10)**	
D 1424	51 (20)	18 (35%)	32 (14)	**1.18 (0.67-2.31)**	$p=0.01$ vs. E1841 [2]
E 1841	33 (14)	6 (18%)	37 (17)	**0.46 (0.20-1.30)**	
R 1933	45 (20)	1 (2%)	60 (ne)	**0.06 (0.02-0.07)**	$p<0.001$ vs. D1424, $p=0.01$ vs. R1165, $p<0.05$ vs. E1841 [2]
R702 substitutions					
p.R702C	18 (9)	16 (89%)	16 (8)	**5.74 (4.40-7.42)**	$p=0.05$ [2]
p.R702H	11 (8)	6 (55%)	21 (8)	**3.08 (1.92-4.72)**	
D1424 substitutions					
p.D1424H	33 (16)	16 (48)	31 (14)	**1.74 (0.90-3.43)**	$p=0.005$ [2]
p.D1424N	13 (6)	0 (0)	ne	**0**	

Notes: only *p* values ≤ 0.05 are reported. [1] = p ≤ 0.008 significance after Bonferroni correction. [2] = p ≤ 0.005 significance after Bonferroni correction.
Abbreviations: ne = not evaluable.

Table 3. Progression of nephropathy to chronic renal failure (CRF) and end-stage renal disease (ESRD) in 54 *MYH9*-RD patients according to the NMMHC-IIA region affected by mutation.

	CRF			**ESRD**		
NMMHC-IIA region (n. of patients)	**Affected patients** (%) [median follow-up, mo.]	**Rate per 100 person year** (95%CI)	***p* value**	**Affected patients** (%) [median follow-up, mo.]	**Rate per 100 person year** (95%CI)	***p* value**
SH1 helix (R702) (n=23)	17 (74%) [48]	19.76 (13.8-28.6)	*p*=0.02	14 (61%) [48]	18.33 (12.43-27.20)	*p*=0.001
Coiled-coil (n=31)	19 (61%) [36]	8.72 (6.04-12.49)		9 (29%) [40]	3.35 (1.55-7.96)	

Abbreviation: mo.= months.

Additional information:
For the mutations in SH1 helix, the age at onset of nephropathy, IRC and ESRD was 19 (SD 9), 23 (16) and 24 (9) years, respectively.
For the mutations in the coiled-coil, the age at onset of nephropathy, IRC and ESRD was 31 (SD 15) 38 (8) and 42 (23) years, respectively.

Table 4 - Correlations between genotype and incidence of sensorineural deafness in 237 *MYH9*-RD patients.

	N. of patients (families)	Affected patients, n (%)	Mean age at onset, years (SD)	**Rate per 100 person year (95% CI)**	***p* values**
NMMHC-IIA domain					
Head	44 (34)	36 (82%)	17 (13)	**5.47 (3.93-1.73)**	*p*<0.001
Tail	193 (83)	78 (40%)	37 (17)	**1.31 (1.01-0.86)**	
NMMHC-IIA region					*p*<0.001
SH3/MD interface	14 (9)	9 (64%)	28 (16)	**3.17 (1.76-5.74)**	*p*=0.01 vs. coiled-coil [1]
SH1 helix (R702)	29 (23)	27 (93%)	13 (9)	**7.76 (5.96-9.93)**	*p*<0.001 vs. all other groups [1]
Coiled-coil	118 (50)	61 (52%)	34 (16)	**1.71 (1.30-2.31)**	
NHT	65 (28)	15 (23%)	53 (17)	**0.71 (0.47-1.11)**	*p*≤0.001 vs. all other groups [1]
NMMHC-IIA residue					*p*<0.001
R 702	29 (23)	27 (93%)	13 (9)	**7.76 (5.96-9.93)**	*p*<0.001 vs. all other groups [2]
R 1165	19 (9)	10 (53%)	26 (13)	**2.34 (1.17-5.61)**	
D 1424	50 (19)	33 (66%)	31 (15)	**2.37 (1.85-3.18)**	
E 1841	30 (14)	13 (43%)	45 (14)	**1.10 (0.64-2.05)**	*p*<0.001 vs. R1165 and D1424 [2]
R 1933	42 (21)	9 (21%)	54 (11)	**0.67 (0.40-1.20)**	*p*<0.001 vs. R1165 and D1424 [2]
R702 substitutions					
p.R702C	18 (17)	17 (94%)	11 (6)	**9.09 (6.68-12.12)**	
p.R702H	10 (6)	9 (90%)	16 (11)	**6.04 (3.88-9.20)**	
D1424 substitutions					
p.D1424H	32 (9)	25 (78%)	32 (16)	**2.73 (2.35-3.20)**	*p*<0.001 [2]
p.D1424N	11 (7)	1 (9%)	50 (ne)	**0.31 (0.10-0.38)**	

Notes: only *p* values ≤ 0.05 are reported. [1] = p ≤ 0.008 significance after Bonferroni correction. [2] = p ≤ 0.005 significance after Bonferroni correction.
Abbreviations: ne = not evaluable.

Table 5 - Correlations between genotype and incidence of cataract in 235 *MYH9*-RD patients.

	N. of patients (families)	Affected patients, %	Mean age at onset, years (SD)	**Rate per 100 person year (95% CI)**	***p* values**
NMMHC-IIA domain					
Head	42 (33)	6 (14%)	33 (16)	**0.57 (0.28-1.32)**	
Tail	193 (83)	37 (19%)	38 (21)	**0.57 (0.39-0.86)**	
NMMHC-IIA region					p=0.002
SH3/MD interface	13 (8)	2 (15%)	52 (6)	**0.49 (0.15-2.44)**	
SH1 helix (R702)	28 (24)	4 (14%)	23 (3)	**0.64 (0.25-2.07)**	
Coiled-coil	119 (51)	31 (26%)	38 (20)	**0.77 (0.52-1.18)**	
NHT	64 (26)	3 (5%)	57 (20)	**0.13 (0.05-0.52)**	*p*<0.001 vs. coiled-coil; *p*=0.001 vs. SH1 helix [1]
NMMHC-IIA residue					*p*<0.001
R 702	28 (24)	4 (14%)	23 (3)	**0.64 (0.25-2.07)**	
R 1165	22 (10)	4 (18%)	45 (23)	**0.55 (0.28-1.22)**	
D 1424	47 (19)	17 (36%)	32 (18)	**1.18 (0.74-2.17)**	*p*<0.05 vs. E1841 [2]
E 1841	31 (13)	7 (23%)	50 (11)	**0.57 (0.27-1.53)**	
R 1933	40 (19)	1 (2%)	75 (ne)	**0.07 (0.02-0.06)**	*p*<0.005 vs. R702, *p*<0.001 vs. D1424, *p*<0.05 vs. R1165 and E1841 [2]
R702 substitutions					
p.R702C	18 (17)	4 (22%)	23 (3)	**1.06 (0.44-3.17)**	
p.R702H	9 (6)	0	ne	**0.00**	
D1424 substitutions					
p.D1424H	29 (10)	13 (45%)	28 (17)	**1.60 (1.18-2.39)**	*p*=0.01 [2]
p.D1424N	12 (8)	0	ne	**0.00**	

Notes: only *p* values ≤ 0.05 are reported. [1] = p ≤ 0.008 significance after Bonferroni correction. [2] = p ≤ 0.005 significance after Bonferroni correction.
Abbreviations: ne = not evaluable.

Table 6. Summary of the risk of occurrence of extra-hematological manifestations of *MYH9*-RD according to seven *MYH9* genotypes.

	Nephropathy	**Deafness**	**Cataracts**
SH3/MD interface substitutions	Low risk	Before age 60 years in all patients	Low risk
R702 substitutions	Before age 40 years in all patients Progression to ESRD in all patients	Before age 40 years in all patients	Low risk
R1165 substitutions	Low risk	Before age 60 years in all patients	Low risk
p.D1424H	High risk Progression to ESRD in a minority of patients	Before age 60 years in all patients	Probably higher risk
p.D1424N	Very low risk	Low risk	Low risk
p.E1841K	Low risk	Low risk	Low risk
NHT deletions	Very low risk	Low risk	Very low risk

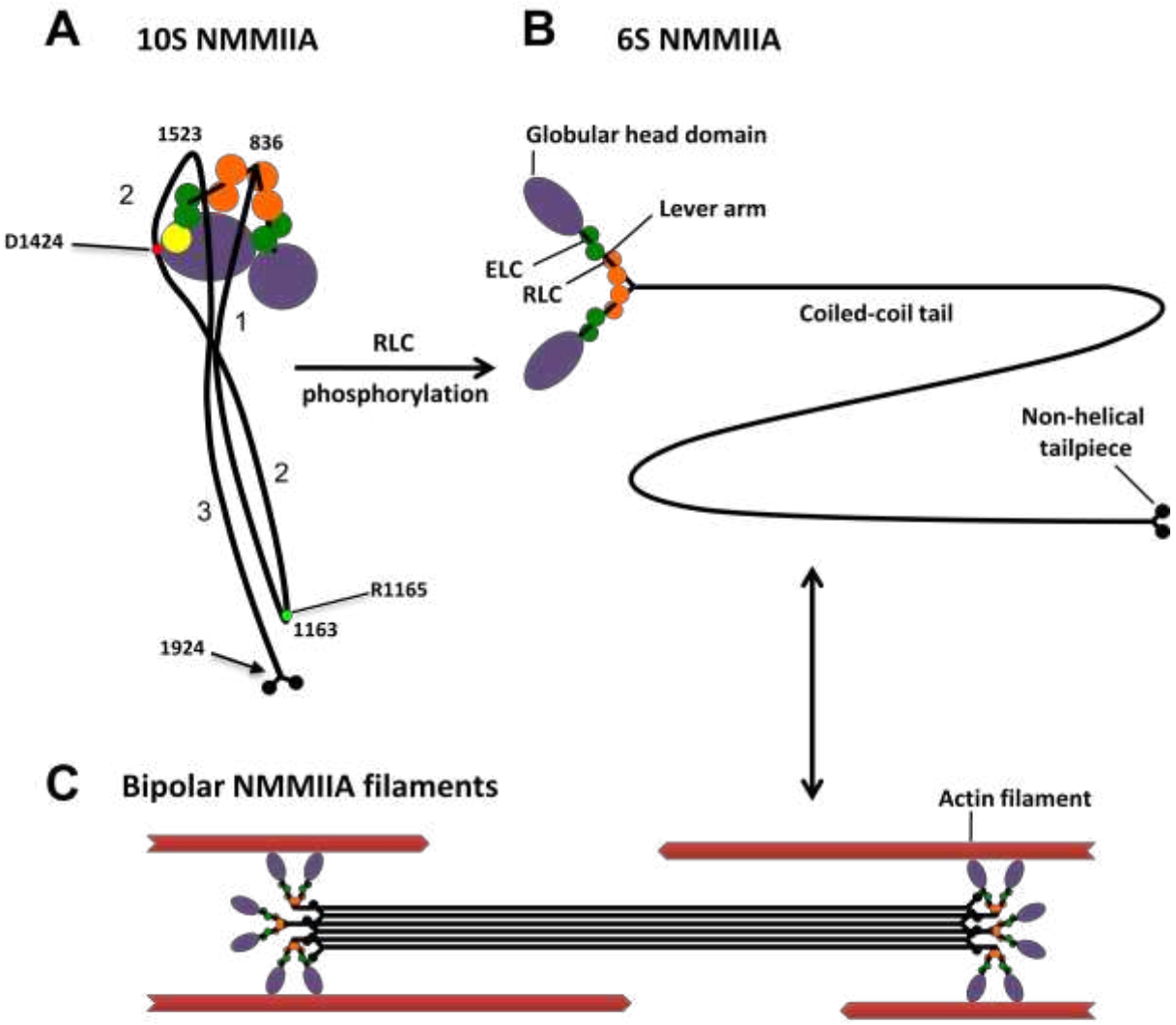

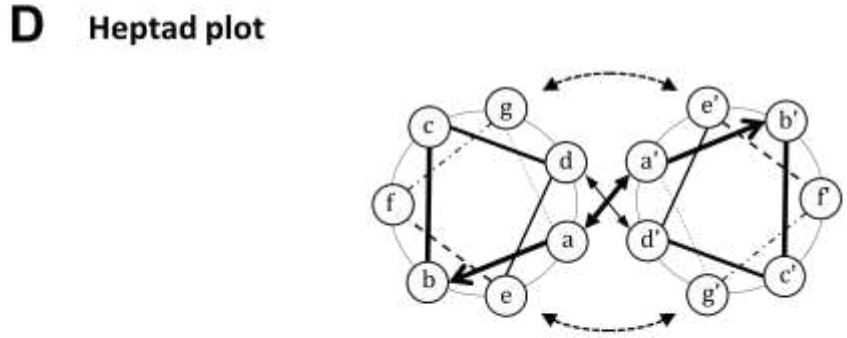

Supporting Figure S1

Supporting Figure S1. Schematic representation of non-muscle myosin IIA (NMM-IIA) domain structure, folding and assembly. (**A**): Diagram of the folded, shut-down 10S conformation of NMM-IIA based on the structure of smooth muscle myosin as seen by negative stain EM (adapted from Burgess et al. 2007). The tail folds into three segments of approximately equal length (numbered 1, 2 and 3). The amino acid residue numbers for the bends are derived assuming homology with smooth muscle myosin. The position of D1424 is indicated (red dot) on tail segment 2: it lies adjacent to the converter subdomain (yellow) of the left head. The R1165 (green dot) is located in a region where the tail forms a sharp bend between segment 1 and 2 in the 10S conformation. Phosphorylation of the regulatory light chain (RLC) causes unfolding of NMM-IIA into the 6S conformation. (**B**): Domain structure of 6S NMM-IIA. The essential light chain (ELC; green) and RLC (orange) bind to the lever arm region of the heavy chain. Two NMM-IIA heavy chains dimerise through their long, C-terminal α-helices to form a coiled-coil tail with a non-helical tail piece at the C-terminus starting at G1924. (**C**): Interactions between the tails of 6S NMM-IIA molecules yield bipolar filaments that function to draw together actin filaments of opposite polarity. (**D**) Heptad plot showing hydrophobic and ionic interactions in the coiled-coil. The sequence is plotted as a helical wheel in which each helix is modified to 3.5 residues per turn such that two turns coincide with one heptad repeat. The resulting paired structure is viewed along the helix axis. Hydrophobic residues in the 'a' and 'd' positions can escape interaction with aqueous solution by forming a hydrophobic seam when the two polypeptide chains associate together (solid arrows). The 'g' and 'e' residues are often charged and can make ionic 'g' to 'e' interactions (shown by the dotted arrows) across the seam, which stabilizes the coiled-coil.

Supporting Figure S2

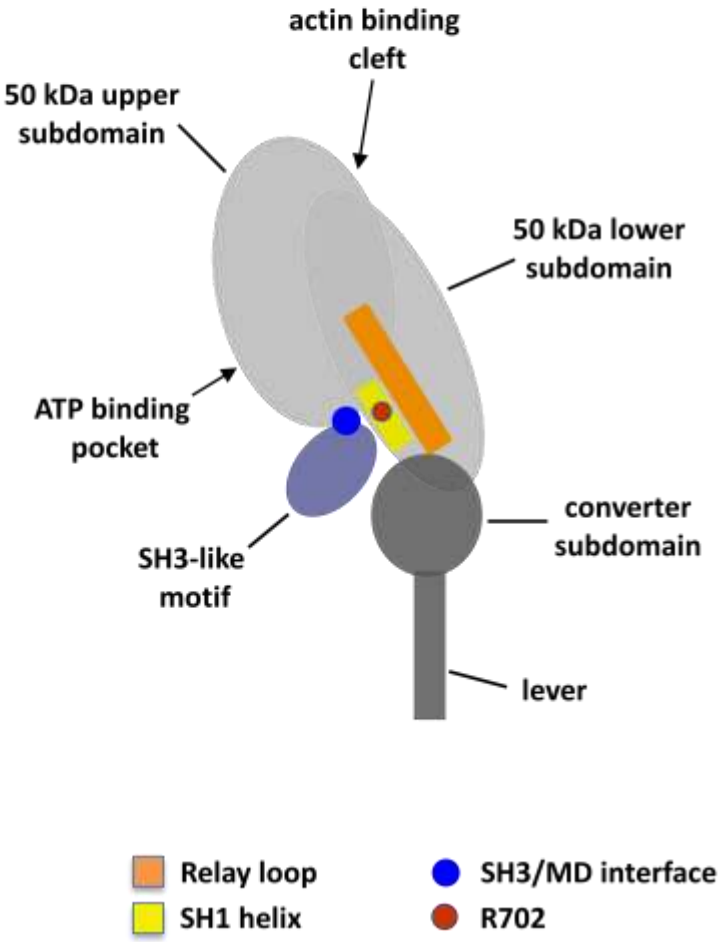

Supporting Figure S2. Schematic representation of the three-dimensional structure of the NMMHC-IIA head domain (HD). The globular head includes four subdomains: from the N- to the C-terminus, they are the SH3-like motif, the upper and the lower 50kDa subdomains, and the converter subdomain. The two 50 kDa subdomains form the so-called motor domain, as it contains the functional regions essential for production of chemomechanical forces. The converter domain connects the lever arm that amplifies the

movement produced by conformational changes of the motor domain. In our case series, the HD mutations were mostly located in two specific regions of the head: a distinct hydrophobic interface between the N-terminal SH3 motif and the 50kDa upper subdomain (SH3/MD interface, blue dot) (Kahr et al., 2009; Dominguez et al. 1998) and at R702 (red dot) localized in the SH1 helix (yellow) of the 50kDa lower subdomain. The relay loop is also schematically represented (see text).

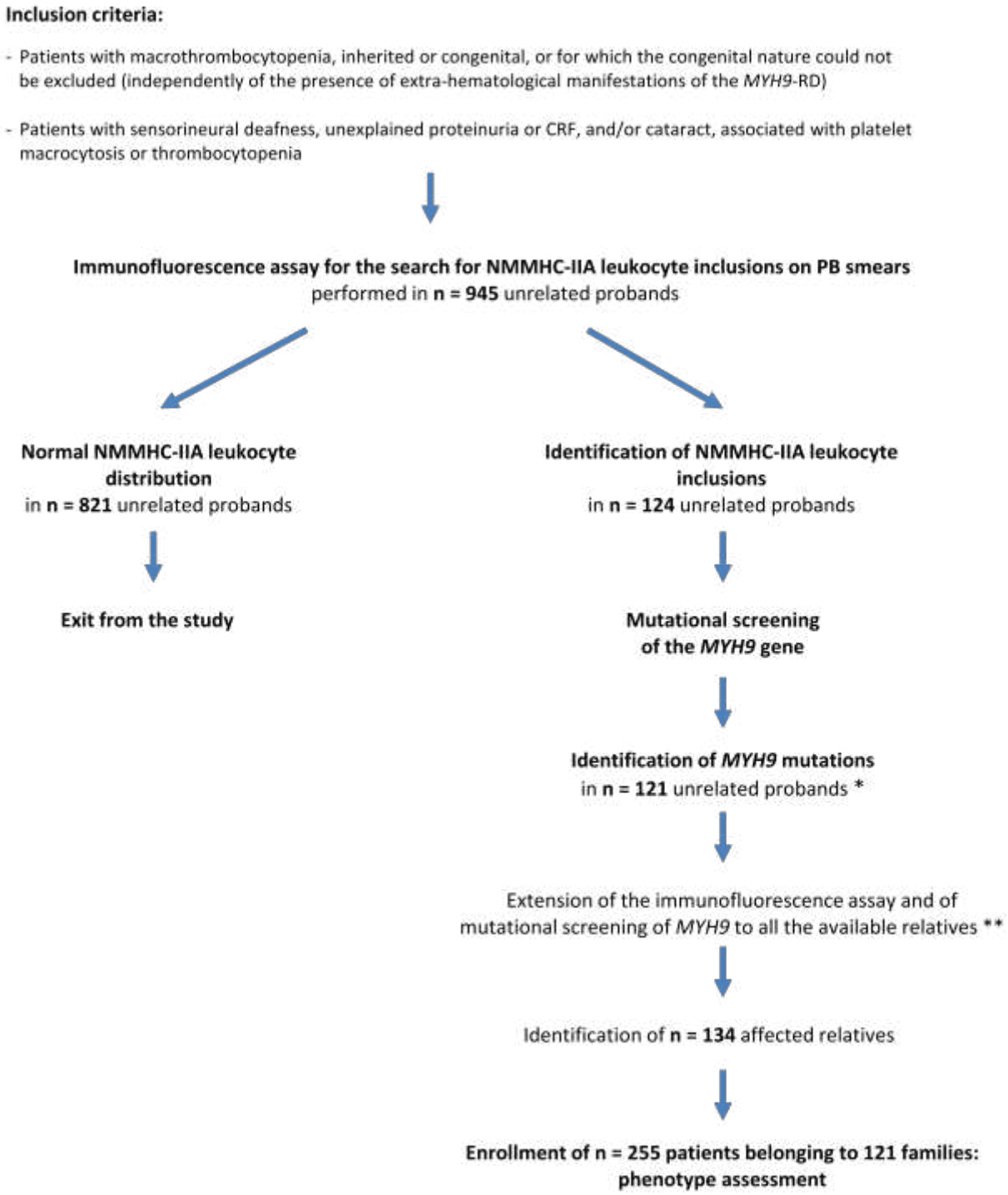

* In 3 probands, no mutation was identified despite the sequencing of all the *MYH9* coding exons including their flanking intronic regions.
** Concordant results derived from the immunofluorescence assay and mutational screening in all investigated individuals.

Abbreviations: PB = peripheral blood

Supporting Figure S3

Supporting Figure S3. Enrollment to this genotype-phenotype study. Patients having the inclusion criteria were identified at the different centers participating in the network of the Italian registry for *MYH9*-RD, whereas the immunofluorescence assay for NMMHC-IIA and molecular screening of *MYH9* were centralized, as detailed in the text.

Supporting Figure S4

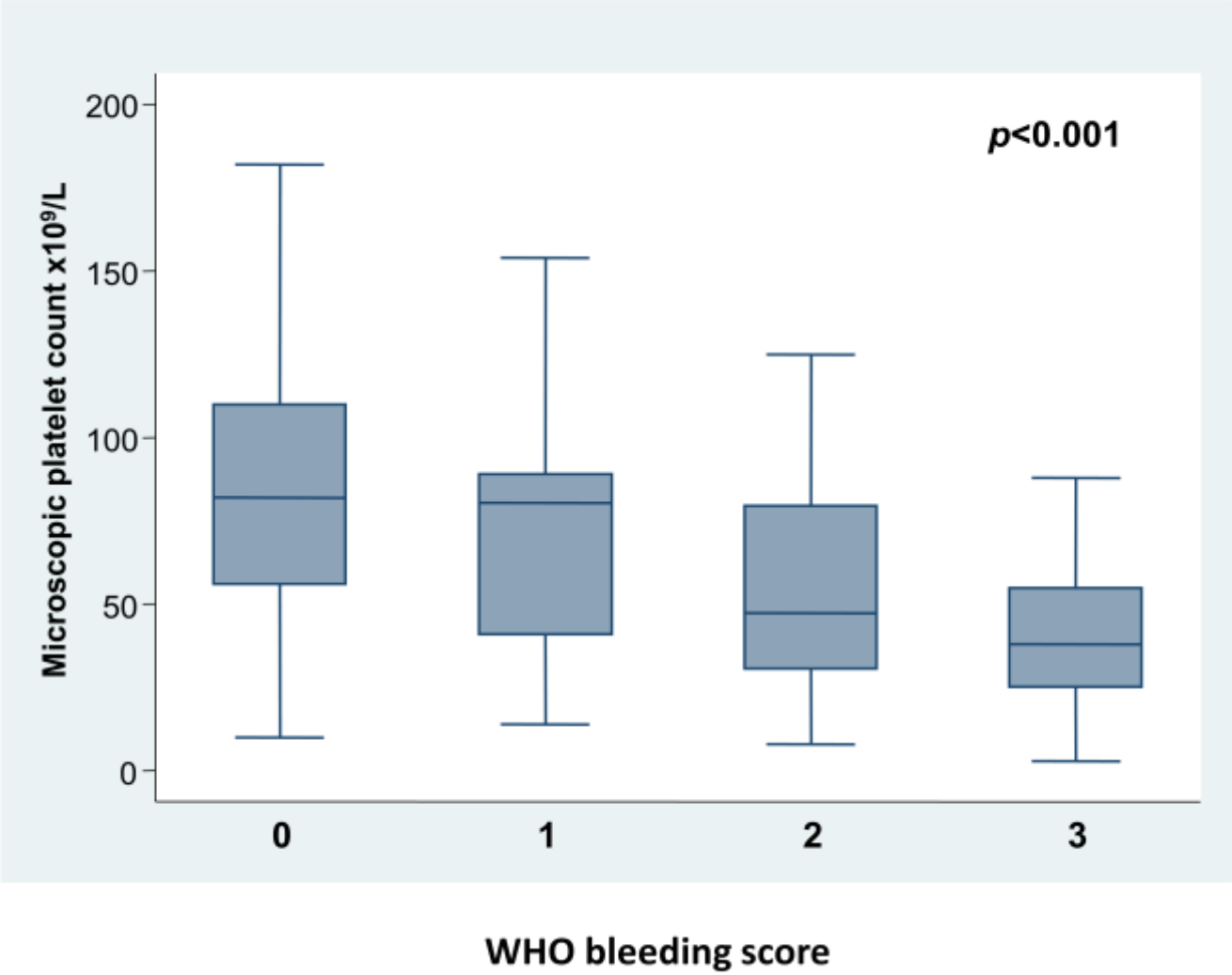

Supporting Figure S4. Correlation between microscopic platelet count and WHO bleeding score. For each WHO bleeding grade, median platelet count (midline), 25^{th}-75^{th} percentiles (box) and extremes (whiskers) are shown.

Supporting Table S1. Occurrence of the extra-hematological complications of the *MYH9*-RD in 255 patients belonging to 121 families.

Family	*MYH9* mutation	N. of patients	Mean age [years] (range)	N. of affected/evaluable patients			
				Nephropathy	ESRD	Deafness	Cataract
1	p.W33C	1	14	0	0	1/1	0
2	p.V34G	3	40 (11-58)	0/3	0/3	2/3	1/3
3	p.N93K	1	46	1/1	0/1	1/1	0/1
4	p.A95D	3	47 (32-75)	0/3	0/3	3/3	0/3
5	p.S96L	1	7	0/1	0/1	0/1	0/1
6	p.S96L	1	4	0/1	0/1	0/1	0/1
7	p.S96L	1	9	0/1	0/1	0/1	0/1
8	p.S96L	2	33 (16-50)	1/2	0/2	2/2	1/2
9	p.S96L	1	4	0/1	0/1	0/1	0/0
10	p.R702C	1	8	1/1	0/1	1/1	0/1
11	p.R702C	1	35	1/1	1/1	1/1	0/1
12	p.R702C	2	29 (27-32)	2/2	1/2	2/2	1/1
13	p.R702C	2	26 (12-40)	1/2	0/1	2/2	0/2
14	p.R702C	1	22	1/1	0/1	1/1	0/1
15	p.R702C	1	21	1/1	1/1	1/1	0/1
16	p.R702C	1	24	1/1	1/1	1/1	1/1
17	p.R702C	1	18	1/1	0/1	1/1	0/1
18	p.R702C	1	22	1/1	1/1	1/1	0/1
19	p.R702C	1	43	1/1	1/1	1/1	0/1
20	p.R702C	1	21	1/1	0/1	1/1	0/1
21	p.R702C	1	4	0/1	0/1	0/1	0/1
22	p.R702C	1	6	1/1	0/1	1/1	0/1
23	p.R702C	1	47	1/1	1/1	1/1	1/1
24	p.R702C	1	20	1/1	1/1	1/1	0/1
25	p.R702C	1	13	0/1	0/1	0/0	0/1
26	p.R702C	1	27	1/1	1/1	1/1	1/1
27	p.R702S	1	44	1/1	0/1	1/1	0/1
28	p.R702H	2	16 (5-28)	1/2	1/2	2/2	0/2
29	p.R702H	2	32 (37-28)	1/2	1/2	1/1	0/1
30	p.R702H	1	26	1/1	1/1	1/1	0/1
31	p.R702H	2	27 (15-40)	1/2	1/2	2/2	0/2
32	p.R702H	2	14 (3-25)	1/2	0/2	2/2	0/1
33	p.R702H	2	26 (1-53)	1/2	1/2	1/2	0/2
34	p.R718W	1	16	1/1	1/1	0/1	0/1
35	p.M847_E853dup	2	19 (6-33)	0/2	0/2	0/2	0/2
36	p.K1048_E1054del	2	27 (10-45)	0/2	0/2	0/2	0/2
37	p.E1066_A1072del	1	25	0/1	0/1	1/1	1/1
38	p.E1066_A1072del	2	19 (1-38)	1/2	0/2	1/2	1/2
39	p.E1066_A1072dup	3	33 (23-51)	0/3	0/3	0/3	1/3
40	p.T1155A	1	16	0/1	0/1	0/1	0/1
41	p.T1155I	1	20 (2-46)	2/4	1/4	1/4	1/4
42	p.R1162T	2	33 (17-50)	0/1	0/2	0/2	0/2
43	p.R1162T	1	28	0/1	0/1	0/1	0/1
44	p.R1165C	4	55 (40-76)	0/3	0/4	2/2	1/3
45	p.R1165C	3	58 (38-82)	0/3	0/3	3/3	0/3
46	p.R1165C	1	14	0/1	0/1	0/1	0/1
47	p.R1165C	2	18 (4-33)	1/2	0/2	0/2	0/2

48	p.R1165C	2	1	0/1	0/1	0/0	0/1
49	p.R1165C	2	26 (13-40)	0/2	0/2	0/2	1/2
50	p.R1165C	4	30 (2-60)	0/3	0/4	0/3	1/4
51	p.R1165C	1	33	0/1	0/1	0/1	0/1
52	p.R1165L	4	24 (14-37)	3/4	0/4	4/4	1/4
53	p.R1165L	1	26	0/1	0/1	1/1	0/1
54	p.D1424H	10	32 (9-63)	2/10	1/10	8/10	6/10
55	p.D1424H	1	41	1/1	1/1	1/1	1/1
56	p.D1424H	5	32 (9-45)	4/5	0/5	5/5	2/5
57	p.D1424H	8	34 (1-56)	5/8	4/8	6/8	2/5
58	p.D1424H	2	42 (30-54)	2/2	0/2	1/1	1/1
59	p.D1424H	2	24 (23-25)	0/2	0/2	1/2	0/2
60	p.D1424H	2	21 (10-32)	1/2	0/2	1/2	1/2
61	p.D1424H	1	62	1/1	0/1	1/1	1/1
62	p.D1424H	2	30 (15-46)	0/2	0/2	1/2	0/2
63	p.D1424N	2	54 (42-67)	0/2	0/2	1/2	0/2
64	p.D1424N	1	35	0/1	0/1	0/1	0/1
65	p.D1424N	1	29	0/1	0/1	0/1	0/1
66	p.D1424N	1	38	0/1	0/1	0/0	0/1
67	p.D1424N	1	48	0/1	0/1	0/1	0/1
68	p.D1424N	3	28 (1-59)	0/3	0/3	0/3	0/3
69	p.D1424N	2	10 (1-21)	0/2	0/2	0/2	0/2
70	p.D1424N	2	16 (7-26)	0/2	0/2	0/1	0/1
71	p.D1424Y	1	58	0/1	0/1	1/1	0/0
72	p.D1424Y	4	50 (34-64)	2/3	0/4	4/4	4/4
73	p.D1424Y	2	29 (9-49)	0/1	0/2	2/2	0/2
74	p.D1447Y	1	20	0/1	0/1	0/1	0/1
75	p.D1447V	4	45 (10-67)	0/4	0/4	3/4	1/4
76	p.D1447V	1	55	1/1	0/1	1/1	1/1
77	p.V1516M	3	36 (23-48)	0/3	0/3	0/3	0/3
78	p.R1557L	2	54 (68-41)	0/2	0/2	1/2	0/2
79	p.E1841K	5	52 (23-81)	0/5	0/5	2/5	1/5
80	p.E1841K	4	46 (23-68)	0/4	0/4	0/4	0/4
81	p.E1841K	1	2	0/1	0/1	0/1	0/1
82	p.E1841K	2	39 (22-56)	0/2	0/2	1/2	0/2
83	p.E1841K	1	33	1/1	0/1	1/1	0/1
84	p.E1841K	2	75 (67-83)	0/2	0/2	1/1	2/2
85	p.E1841K	1	35	0/1	0/1	0/0	0/0
86	p.E1841K	5	41 (22-72)	2/5	0/5	2/4	1/4
87	p.E1841K	1	28	0/1	0/1	0/1	0/1
88	p.E1841K	1	27	0/1	0/1	0/1	0/1
89	p.E1841K	1	43	0/1	0/1	0/1	0/1
90	p.E1841K	1	73	1/1	1/1	1/1	0/1
91	p.E1841K	7	38 (18-73)	2/7	1/7	5/7	3/7
92	p.E1841K	1	10	0/1	0/1	0/1	0/1
93	p.E1841K	1	52	0/1	0/1	0/0	0/0
94	p.G1924Rfs*21	3	37 (22-46)	0/3	0/3	0/3	0/3
95	p.D1925Tfs*23	5	29 (2-61)	1/5	1/5	1/5	0/5
96	p.V1930Cfs*18	4	70 (45-87)	0/4	0/4	2/3	1/4
97	p.R1933*	5	52 (28-68)	1/5	0/5	1/4	0/4
98	p.R1933*	4	38 (12-64)	0/4	0/4	0/4	0/4
99	p.R1933*	2	42 (30-55)	0/2	0/2	0/1	0/0
100	p.R1933*	2	26 (12-40)	0/2	0/2	0/2	0/0
101	p.R1933*	1	32	0/1	0/1	0/1	0/1
102	p.R1933*	3	47 (35-68)	0/3	0/3	1/3	0/3
103	p.R1933*	2	36 (29-43)	0/2	0/2	1/2	0/1

104	p.R1933*	1	54	0/1	0/1	1/1	0/1
105	p.R1933*	2	22 (8-37)	0/2	0/2	0/2	0/1
106	p.R1933*	3	16 (1-34)	0/3	0/3	1/3	0/3
107	p.R1933*	2	34 (21-48)	0/2	0/2	0/1	0/2
108	p.R1933*	3	41 (17-56)	0/3	0/3	2/3	0/3
109	p.R1933*	1	18	0/1	0/1	0/1	0/1
110	p.R1933*	1	22	0/1	0/1	0/1	0/1
111	p.R1933*	2	22 (5-39)	0/2	0/2	0/2	0/2
112	p.R1933*	1	11	0/1	0/1	0/1	0/1
113	p.R1933*	2	22 (7-38)	0/2	0/2	0/1	0/1
114	p.R1933*	1	22	0/0	0/1	0/1	0/1
115	p.R1933*	2	12 (3-22)	0/2	0/2	0/2	0/2
116	p.R1933*	4	47 (1-82)	0/4	0/4	2/4	1/4
117	p.R1933Efs*15	2	37 (25-49)	0/2	0/2	0/2	0/2
118	p.M1934Wfs*14	2	19 (2-37)	0/2	0/2	1/2	1/2
119	p.D1941Mfs*7	3	27 (17-42)	1/3	1/3	1/3	0/3
120	p.D1941Mfs*7	2	32 (17-47)	0/2	0/2	0/2	0/2
121	p.E1945*	5	28 (2-63)	0/5	0/5	0/5	0/5

Abbreviations: ESRD= end-stage renal disease.

Supporting Table S2. Clinical presentation of 221 patients with *MYH9*-RD who were investigated for macrothrombocytopenia, sensorineural deafness, proteinuric nephropathy, and cataract (mean age at evaluation, 35 years).

Clinical picture	N. of patients (%)		Mean age [yrs.]
Isolated MTCP *	108	(48.9%)	25
MTCP ** + deafness	40	(18.1%)	41
MTCP + nephropathy	4	(1.8%)	20
MTCP + cataracts	3	(1.4%)	27
MTCP + deafness + nephropathy	30	(13.6%)	33
MTCP + deafness + cataracts	16	(7.2%)	47
MTCP + nephropathy + cataracts	1	(0.4%)	2
MTCP + deafness + nephropathy + cataracts	19	(8.6%)	44

Notes: * in three patients phase-contrast microscopy revealed platelet count at the lower limit of the normal range associated with platelet macrocytosis; ** in two patients phase-contrast microscopy revealed platelet count at the lower limit of the normal range associated with platelet macrocytosis.
Abbreviations: MTCP = macrothrombocytopenia.

Supporting Table S3. Correlations between genotype and platelet count as determined by phase contrast microscopy in 167 *MYH9*-RD patients.

	N. of patients	**Median platelet count (IQR), x10^9/L**	***p* value**
NMMHC-IIA domain			
Head	35	**30 (24-42)**	$p<0.001$
Tail	132	**80 (55-100)**	
NMMHC-IIA region			$p<0.001$
SH3/MD interface	13	**30 (25-48)**	$p<0.001$ vs. coiled-coil and NHT [1]
SH1 helix (R702)	21	**27 (24-37)**	$p<0.001$ vs. coiled-coil and NHT [1]
Coiled-coil	81	**71 (49-95)**	
NHT	44	**88 (75-102)**	

Notes: only *p* values ≤ 0.05 are reported. [1] = p ≤ 0.008 significance after Bonferroni correction.

Supporting Table S4. Correlations between genotype and WHO bleeding score in 183 *MYH9*-RD patients.

	N. of patients	**Median platelet count, 10^9/L (IQR)** [evaluable patients]	**Median WHO bleeding grade (IQR)**	***p* value**	**% of patients with grade 2 / 3**	***p* value** [a]
NMMHC-IIA domain						
Head	32	27 (21-41) [29]	**2 (0.5-3)**	*p*<0.001	**34 / 28**	p<0.001
Tail	151	80 (55-100) [116]	**0 (0-1)**		**16 / 5**	
NMMHC-IIA region				*p*<0.001		*p*<0.001
SH3/MD interface	13	30 (21-49) [13]	**2 (0-3)**	*p*=0.03 vs. coiled-coil and *p*=0.02 vs. NHT [1]	**38 / 31**	*p*=0.03 vs. coiled-coil and p<0.001 vs. NHT [1]
SH1 helix (R702)	18	25 (17-37) [15]	**2 (1-3)**	*p*<0.001 vs. coiled-coil and NHT [1]	**33 / 28**	*p*<0.001 vs. coiled-coil and NHT [1]
Coiled-coil	84	70 (47-95) [68]	**0 (0-1)**		**13 / 6**	
NHT	57	90 (67-102) [39]	**0 (0-1)**		**19 / 2**	

Notes: only *p* values ≤ 0.05 are reported. [1] = p ≤ 0.008 significance after Bonferroni correction.

[a]= comparison of the number of patients with WHO grade 0 or 1 vs. WHO grade 2 or 3.